

# ReLU Neural Networks with Linear Layers are Biased Towards Single- and Multi-Index Models

Suzanna Parkinson\*      Greg Ongie†      Rebecca Willett‡

June 25, 2024

## Abstract

Neural networks often operate in the overparameterized regime, in which there are far more parameters than training samples, allowing the training data to be fit perfectly. That is, training the network effectively learns an interpolating function, and properties of the interpolant affect predictions the network will make on new samples. This manuscript explores how properties of such functions learned by neural networks of depth greater than two layers. Our framework considers a family of networks of varying depths that all have the same *capacity* but different *representation costs*. The representation cost of a function induced by a neural network architecture is the minimum sum of squared weights needed for the network to represent the function; it reflects the function space bias associated with the architecture. Our results show that adding additional linear layers to the input side of a shallow ReLU network yields a representation cost favoring functions with low *mixed variation* – that is, it has limited variation in directions orthogonal to a low-dimensional subspace and can be well approximated by a single- or multi-index model. Such functions may be represented by the composition of a function with low two-layer representation cost and a low-rank linear operator. Our experiments confirm this behavior in standard network training regimes. They additionally show that linear layers can improve generalization and the learned network is well-aligned with the true latent low-dimensional linear subspace when data is generated using a multi-index model.

## 1 Introduction

An outstanding problem in understanding the generalization properties of overparameterized neural networks is characterizing the inductive bias of various architectures – i.e., characterizing the types of predictors learned when training networks with the capacity to represent large families of functions. Past work has explored this problem through the lens of *representation costs*. Specifically, the representation cost of a function  $f$  is the minimum sum of squared network weights necessary for the network to represent  $f$ . Representation costs are key to understanding how overparameterized neural networks trained with limited data are able to generalize well. For instance, imagine training a neural network to interpolate a set of training samples using weight decay regularization

---

\*Committee on Computational and Applied Mathematics, University of Chicago, Chicago, IL (email: sueparkinson@uchicago.edu).

†Department of Mathematical and Statistical Sciences, Marquette University, Milwaukee, WI (email: gregory.ongie@marquette.edu).

‡Department of Statistics, Department of Computer Science, and Committee on Computational and Applied Mathematics, University of Chicago, Chicago, IL.

(i.e.,  $\ell^2$ -regularization on the network weights); the corresponding interpolant will have low representation cost. Different network architectures are associated with different representation costs, so the network architecture will influence which interpolating function is learned, which can have a profound effect on test performance. The following key question then arises: *How does network architecture affect which functions have minimum representation cost?*

In this paper, we describe the representation cost associated with deep fully-connected networks having  $L$  layers in which the first  $L - 1$  layers have linear activations and the final layer has a ReLU activation. As detailed in Section 1.1, networks related to this class play an important role in both theoretical studies of neural network generalization properties and experimental efforts. This is a particularly important family to study because adding linear layers does not change the capacity or expressivity of a network, even though the number of parameters may change. This means that different behaviors for networks of different depths solely reflect the role of depth and not of capacity. *In effect, this framework isolates the effects of depth from those of expressivity.*

We show that adding linear layers to a ReLU network while using  $\ell_2$ -regularization (weight decay) is equivalent to fitting a two-layer ReLU network with nuclear or Schatten norm regularization on the innermost weight matrix and  $\ell^2$  norm regularization on the outermost weights. The associated function space inductive bias corresponds to a notion of latent low-dimension structure that has close connections to multi- and single-index models, as illustrated in Figure 1. Specifically, we relate the function space inductive bias to the singular value spectrum of the expected gradient outer product (EGOP) matrix, where gradients are taken with respect to the neural network inputs. We prove that the representation cost is bounded in terms of the *mixed variation* and *index rank* of a function, which are properties defined in terms of the EGOP singular values. Our bounds imply that networks minimizing the representation cost must have an EGOP with low effective rank, where the rank decreases as more linear layers are added. Our numerical experiments on synthetic data show that with a moderate number of linear layers, the principal subspace of the learned function’s EGOP is low-dimensional and closely approximate the principal subspace of the data-generating function’s EGOP, which improves in- and out-of-distribution generalization.

**Contributions** Our theoretical results show that adding linear layers to a shallow ReLU network trained with weight decay regularization results in global minimizers with low-dimensional structure, and empirically, the phenomenon persists in practical training settings in which we may not find the global minimizer. These theoretical results do not depend on the data-generating function having low-dimensional structure, contrary to past work focused on learning single- and multi-index models. Furthermore, when the data-generating function has approximate low-dimensional structure and the sample size is moderate, linear layers improve generalization in our experiments.

More specifically, this manuscript makes the following contributions:

- Formalizes the notions of the mixed variation and index rank of a function, establishing connections with single- and multi-index models.
- Characterizes the representation cost as a function of the number of linear layers, and bounds this cost in terms of the function’s mixed variation and index rank.
- Bounds the effective index rank of models that interpolate data with minimal representation cost.

- Demonstrates empirically that training models with linear layers using standard training and optimization approaches yields models with low effective index rank and strong generalization performance. That is, linear layers are a useful form of regularization that promotes low-rank structure, which in turn can improve generalization.

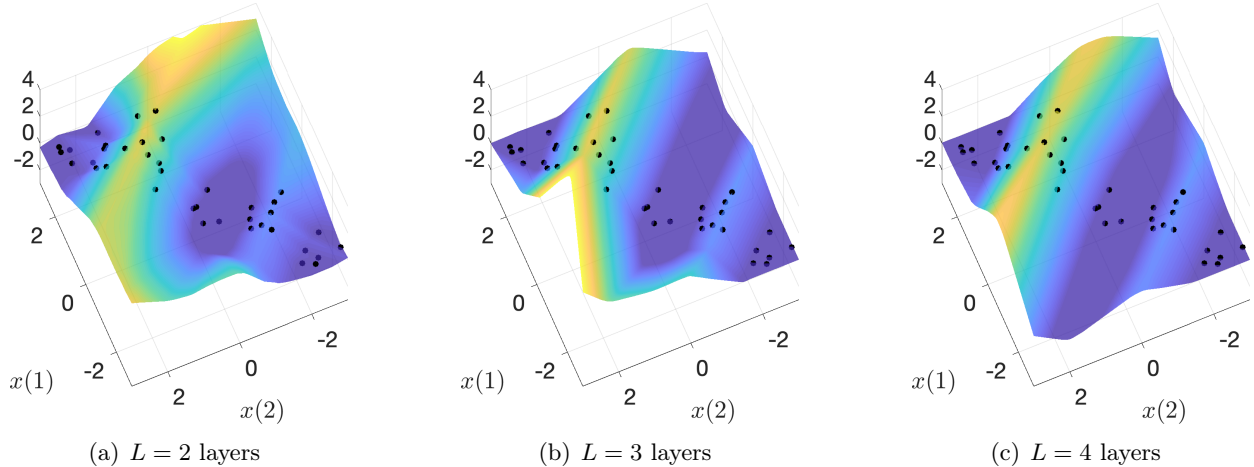


Figure 1: **Numerical evidence that weight decay promotes unit alignment with more linear layers.** Neural networks with  $L - 1$  linear layers followed by one ReLU layer were trained using SGD with  $\ell_2$ -regularization (weight decay) to close to zero training loss on the training samples, as shown in black. Pictured in (a)-(c) are the resulting interpolating functions shown as surface plots. Our theory predicts that as the number of linear layers increases, the learned interpolating function will become closer to constant in directions orthogonal to a low-dimensional subspace on which a parsimonious interpolant can be defined.

## 1.1 Related work

**Representation costs** In neural networks, it has been argued that “the size [magnitude] of the weights is more important than the size [number of weights or parameters] of the network” [1], an idea reinforced by [2, 3] and yielding insight into the generalization performance of overparameterized neural networks [4, 5, 6, 7]. Networks trained with weight decay regularization seek weights with minimal norm required to represent a function that accurately fits the training data. Therefore, minimal norm solutions and the corresponding *representation cost* of a function play an important role in generalization performance.

The representation costs associated with shallow (i.e., two-layer) networks have been studied extensively. In [8], Bach studies the variation norm, which corresponds to the representation cost associated with infinitely wide two-layer networks. Savarese et al. [9] and Boursier and Flammarion [10] provide a function space description of representation cost of univariate functions in the case of two-layer ReLU networks; Ongie et al. [11] extends this analysis to scalar-valued multivariate functions, while Shenouda et al. [12] consider the case of vector-valued outputs. Parhi and Nowak [13], Bartolucci et al. [14], and Unser [15] provide representer theorems, which show that for a class of variational problems regularized using the infinite-width two-layer representation cost there exist solutions realizable as finite-width ReLU networks. A line of work from Ergen and Pilanci explores the connection between two-layer representation costs and convex formulations of network

training [16, 17, 18]. Work by Mulayoff et al. [19] and Nacson et al. [20] connects the function space representation costs of two-layer ReLU networks to the stability of SGD minimizers.

There have also been several efforts to understand the representation costs of deep non-linear networks. Notably, Parhi and Nowak [21] examine deep ReLU networks with one additional *linear* layer between ReLU layers, and relate the corresponding representation cost to a compositional version of the two-layer representation cost; however, an explicit characterization of the associated function space inductive bias is not given in this work. Jacot [22, 23] connects the representation costs of deep ReLU networks in the limit as the number of layers goes to infinity with certain notions of nonlinear function rank; see Section 3.1 for more discussion. Ergen and Pilanci [18] characterize representation cost minimizers associated with deep nonlinear networks, but places strong assumptions on the data distribution (i.e., rank-1 or orthonormal training data). Additionally, recent work studies representation cost minimizers in the context of parallel deep ReLU architectures [24], depth-4 networks on one-dimensional data [25], and path-norm regularization in place of  $\ell^2$ -regularization [26].

**Linear layers** The inductive bias associated with fitting deep *linear* networks have been studied extensively. Gunasekar et al. [27] show that  $L$ -layer linear networks with diagonal structure (i.e., all weight matrices are diagonal) induces a non-convex implicit regularization over network weights corresponding to the  $\ell^q$  norm of the outer layer weights for  $q = 2/L$ , and similar conclusions hold for deep linear convolutional networks. Wang et al. [24] show that for deep, fully-connected linear networks the associated representation cost reduces to the Schatten- $q$  penalty on a virtual single hidden layer weight matrix. Additionally, Dai et al. [28] examine the representation costs of deep linear networks under various connectivity constraints from a function space perspective, and Ji and Telgarsky [29] study the gradient descent path of deep linear networks.

The role of linear layers in *nonlinear* networks has also been explored in a number of works. In [30], Golubeva et al. study the role of network width when the number of parameters is held fixed; they specifically look at increasing the width without increasing the number of parameters by adding linear layers. This procedure seems to help with generalization performance (as long as the training error is controlled). Khodak et al. [31] study how to initialize and regularize linear layers in nonlinear networks and conclude that low-rank structure emerges empirically. One of the main contributions of this paper is an understanding of why this low-rank structure emerges and how it can improve generalization.

The effect of linear layers on training speed was previously examined by Ba and Caruana [32] and Urban et al. [33]. Arora et al. consider implicit acceleration in deep nets and claim that depth induces a momentum-like term in training deep linear networks with SGD [34]. The implicit regularization of gradient descent has been studied in the context of matrix and tensor factorization problems [35, 27, 36, 37]. Similar to this work, low-rank representations play a key role in their analysis. Linear layers have also been shown to help uncover latent low-dimensional structure in dynamical systems [38].

**Single- and multi-index models** Multi-index models are functions of the form

$$f(\mathbf{x}) = g(\langle \mathbf{v}_1, \mathbf{x} \rangle, \langle \mathbf{v}_2, \mathbf{x} \rangle, \dots, \langle \mathbf{v}_r, \mathbf{x} \rangle) = g(\mathbf{V}^\top \mathbf{x}) \quad (1)$$

for  $\mathbf{x} \in \mathbb{R}^d$ , for some matrix  $\mathbf{V} := [\mathbf{v}_1 \ \dots \ \mathbf{v}_r] \in \mathbb{R}^{d \times r}$  with linearly independent columns, and an unknown *link function*  $g : \mathbb{R}^r \rightarrow \mathbb{R}^D$ . The  $r$ -dimensional subspace spanned by the columns of  $\mathbf{V}$  is

often called the *central subspace* associated with  $f$ . Single-index models correspond to the special case where  $r = 1$ . (Like most work on single-index models, in this paper we assume that the output dimension  $D = 1$ , but we generalize to the case that  $D > 1$  in Appendix C.) Multiple works have explored learning such models (i.e., learning both the central subspace and the link function) in high dimensions [8, 39, 40, 41, 42, 43, 44, 45, 46]. The link function  $g$  has an  $r$ -dimensional domain, so the sample complexity of learning these models depends primarily on  $r$  even when the dimension  $d$  of the inputs is large. As noted in [43], the minimax mean squared error rate for general functions  $f$  defined on a  $d$ -dimensional input space that are  $s$ -Hölder smooth is  $n^{-\frac{2s}{2s+d}}$ , while for functions with a rank- $r$  central subspace, the minimax rate is  $n^{-\frac{2s}{2s+r}}$ . The difference between these rates implies that for  $r \ll d$ , a method that can adapt to the central subspace can achieve far smaller function estimation errors (and hence better generalization) than a non-adaptive method.

Several recent papers [8, 47, 48, 49, 50] provide bounds on generalization errors when learning single- and multi-index models using shallow neural networks. Bach [8] describes learning single- or multi-index models in a function space optimization framework with the two-layer representation cost serving as a regularizer, while Damien et al. [48], Bietti et al. [47], and Mousavi et al. [49] focus on shallow networks trained via specialized variations of gradient descent or gradient flow. Contrary to the present paper, some of these works explicitly enforce single-index structure during training: Bietti et al. [47] by constraining the inner weights of all hidden nodes to have the same weight vector, and Mousavi-Hosseini et al. [49] by initializing all weights to be equal and noting that gradient-based updates of the weights will maintain this symmetry. Finally, as a negative result, Ardeshir et al. [50] prove that two-layer ReLU networks regularized with the two-layer representation cost are not well-suited to learning the parity function, which is a single-index model, suggesting that the inductive bias of the two-layer representation cost is incompatible with learning certain types of single-index models.

**Expected Gradient Outer Products (EGOP) of neural networks** There are several empirical works highlighting low-rank structures emerging during the training of overparameterized neural networks and hypothesizing about the role of this structure in the generalization performance of overparameterized models [51, 31, 52]. For example, Radhakrishnan et al. [52] examine the Expected Gradient Outer Product (EGOP) of a fitted model; specifically, for a model  $f(\mathbf{x})$  the EGOP is

$$\mathbb{E}_X[\nabla f(X)\nabla f(X)^\top]. \quad (2)$$

Their empirical study highlights how the EGOP of trained neural networks correlates with features salient to the learning task. Our work theoretically characterizes how the EGOP is influenced by linear layers in the network. Further connections between the EGOP and neural network models are explored in [53, 54]. The EGOP is also central to the active subspaces dimensionality reduction technique [55, 56], and was originally studied in the context of multi-index regression [57, 58, 59, 60, 61].

## 1.2 Outline

In Section 2 we formally define the neural network architectures we study and their representation costs. In Section 3 we define the index rank and mixed variation of a function. Our main theoretical results are in Section 4, where we connect the representation cost with index rank and mixed variation. The numerical experiments in Section 5 show that our theory is predictive of practice

when the data comes from a low-index-rank function. We discuss the implications and limitations of our results in Section 6. Another expression for the representation cost can be found in Appendix A. Most technical details are reserved for the remainder of the appendix. Of note, a generalization of the results to vector-valued functions can be found in Appendix C.

### 1.3 Notation

For a vector  $\mathbf{a} \in \mathbb{R}^K$ , we use  $\|\mathbf{a}\|_p$  to denote its  $\ell^p$  norm and  $a_k$  to denote the  $k$ -th entry. For a matrix  $\mathbf{W}$ , we use  $\|\mathbf{W}\|_{op}$  to denote the operator norm,  $\|\mathbf{W}\|_F$  to denote the Frobenius norm,  $\|\mathbf{W}\|_*$  to denote the nuclear norm (i.e., the sum of the singular values), and for  $q > 0$  we use  $\|\mathbf{W}\|_{S^q}$  to denote the Schatten- $q$  quasi-norm (i.e., the  $\ell^q$  quasi-norm of the singular values of  $\mathbf{W}$ ). We let  $\sigma_k(\mathbf{W})$  denote the  $k$ -th largest singular value of  $\mathbf{W}$  and  $\mathbf{w}_k$  denote row  $k$  of  $\mathbf{W}$ . Given a vector  $\boldsymbol{\lambda} \in \mathbb{R}^K$ , the matrix  $\mathbf{D}_{\boldsymbol{\lambda}} \in \mathbb{R}^{K \times K}$  is a diagonal matrix with the entries of  $\boldsymbol{\lambda}$  along the diagonal. We write  $\boldsymbol{\lambda} > 0$  to indicate that  $\boldsymbol{\lambda}$  has all positive entries. For the weighted  $L_2$ -norm of a function  $f : \mathbb{R}^d \rightarrow \mathbb{R}$  with respect to a probability distribution  $\rho$  we write  $\|f\|_{L_2(\rho)}$ . We use  $N(\mu, \sigma^2)$  for the normal distribution with mean  $\mu$  and standard deviation  $\sigma$  and  $U(\Omega)$  for the uniform distribution over a set  $\Omega$ . Finally, we use  $[t]_+ = \max\{0, t\}$  to denote the ReLU activation, whose application to vectors is understood entrywise.

## 2 Problem Formulation

Let  $\mathcal{X} \subseteq \mathbb{R}^d$  be either a bounded convex set with a nonempty interior or all of  $\mathbb{R}^d$ . Let  $\mathcal{N}_2(\mathcal{X})$  denote the space of functions  $f : \mathcal{X} \rightarrow \mathbb{R}$  expressible as a two-layer ReLU network having input dimension  $d$ ; we allow the width  $K$  of the single hidden layer to be unbounded. Every function in  $\mathcal{N}_2(\mathcal{X})$  is described (non-uniquely) by a collection of weights  $\theta = (\mathbf{W}, \mathbf{a}, \mathbf{b}, c)$ :

$$h_{\theta}^{(2)}(\mathbf{x}) = \mathbf{a}^{\top} [\mathbf{W}\mathbf{x} + \mathbf{b}]_+ + c = \sum_{k=1}^K a_k [\mathbf{w}_k^{\top} \mathbf{x} + b_k]_+ + c \quad (3)$$

for some  $K \in \mathbb{N}$ ,  $\mathbf{W} \in \mathbb{R}^{K \times d}$ ,  $\mathbf{a} \in \mathbb{R}^K$ ,  $\mathbf{b} \in \mathbb{R}^K$ , and  $c \in \mathbb{R}$ . We denote the set of all such parameter vectors  $\theta$  by  $\Theta_2$ .

In this work, we consider a re-parameterization of networks in  $\mathcal{N}_2(\mathcal{X})$ . Specifically, we replace the linear input layer  $\mathbf{W}$  with  $L - 1$  linear layers:

$$h_{\theta}^{(L)}(\mathbf{x}) = \mathbf{a}^{\top} [\mathbf{W}_{L-1} \cdots \mathbf{W}_2 \mathbf{W}_1 \mathbf{x} + \mathbf{b}]_+ + c \quad (4)$$

where now  $\theta = (\mathbf{W}_1, \mathbf{W}_2, \dots, \mathbf{W}_{L-1}, \mathbf{a}, \mathbf{b}, c)$ . Again, we allow the widths of all layers to be arbitrarily large. Let  $\Theta_L$  denote the set of all such parameter vectors. With any  $\theta \in \Theta_L$  we associate the  $\ell_2$ -regularization penalty:

$$C_L(\theta) = \frac{1}{L} (\|\mathbf{a}\|_2^2 + \|\mathbf{W}_1\|_F^2 + \cdots + \|\mathbf{W}_{L-1}\|_F^2), \quad (5)$$

i.e., the squared Euclidean norm of all non-bias weights<sup>1</sup>. This type of regularization penalty is also

---

<sup>1</sup>Similar to [11], we do not regularize the bias terms in our definition of the cost  $C_L$ . This simplifies the theoretical analysis; for example, our formulation makes the representation cost translation invariant, a property that is lost when one regularizes the bias terms. However, we believe that regularizing biases will not substantively change the resulting inductive bias. For example, as shown in [10], regularizing the biases in a 2-layer network results in a weighted version of the usual representation cost formulas.

known as *weight decay* in the machine learning literature [62, 63].

Given training pairs  $\{(\mathbf{x}_i, y_i)\}_{i=1}^n$  with  $\mathbf{x}_i \in \mathcal{X}$  and  $y_i \in \mathbb{R}$ , and a loss function  $\ell(\cdot, \cdot) : \mathbb{R} \times \mathbb{R} \rightarrow [0, \infty)$ , consider the problem of finding an  $L$ -layer network that minimizes the  $\ell^2$ -regularized empirical risk:

$$\min_{\theta \in \Theta_L} \frac{1}{n} \sum_{i=1}^n \ell(h_\theta^{(L)}(\mathbf{x}_i), y_i) + \lambda C_L(\theta), \quad (6)$$

where  $\lambda > 0$  is a regularization parameter. We may recast (6) as an optimization problem in function space: for any  $f \in \mathcal{N}_2(\mathcal{X})$ , define its  $L$ -layer *representation cost*  $R_L(f)$  by

$$R_L(f) = \inf_{\theta \in \Theta_L} C_L(\theta) \quad \text{s.t.} \quad f = h_\theta^{(L)}|_{\mathcal{X}}. \quad (7)$$

Then (6) is equivalent to the function space optimization problem

$$\min_{f \in \mathcal{N}_2(\mathcal{X})} \frac{1}{n} \sum_{i=1}^n \ell(f(\mathbf{x}_i), y_i) + \lambda R_L(f). \quad (8)$$

Therefore,  $R_L$  is the function space regularizer induced by the parameter space regularizer  $C_L$ .

Earlier work, such as [9], has shown that the 2-layer representation cost reduces to

$$R_2(f) = \inf_{\theta \in \Theta_2} \sum_{k=1}^K |a_k| \quad \text{s.t.} \quad \|\mathbf{w}_k\|_2 = 1, \quad \forall k \in [K] \quad \text{and} \quad f = h_\theta^{(2)}. \quad (9)$$

*One goal of this paper is to characterize the representation cost  $R_L$  for different numbers of linear layers  $L \geq 3$ , and identify which functions have low  $R_L$  cost.*

In practice, the regularization strength parameter  $\lambda$  in (8) is often taken to be sufficiently small that the empirical risk dominates the overall cost during the early phases of training. In this case, any minimizer  $f$  of (8) will satisfy  $\ell(f(\mathbf{x}_i), y_i) \approx 0$  for all  $i \in [n]$ . Assuming this implies  $f(\mathbf{x}_i) \approx y_i$ , we see that  $f$  approximately interpolates the training data while achieving low  $R_L$  cost. This motivates us to consider the minimum  $R_L$  cost interpolation problem:

$$\min_{f \in \mathcal{N}_2(\mathcal{X})} R_L(f) \quad \text{s.t.} \quad f(\mathbf{x}_i) = y_i \quad \forall i \in [n]. \quad (10)$$

Informally, (10) can be thought of as the limit of (8) as the regularization strength  $\lambda \rightarrow 0$ . *Another goal of this paper is to describe how the set of global minimizers to (10) changes with  $L$ , providing insight into the role of linear layers in nonlinear ReLU networks.*

### 3 Index rank and mixed variation

We will see that adding linear layers induces a representation cost that favors functions well-approximated by a low-dimensional multi-index model, in which case we say the function has low *index rank* or low *mixed variation*. In this section, we formalize the notions of the index rank and the mixed variation of a function as well as their connections to related concepts in the literature.

### 3.1 Low-index-rank functions

We define the index rank of a function using its expected gradient outer product (EGOP), a tool used in *multi-index regression* [57, 58, 59, 60, 61] as well as the *active subspaces* literature [56, 55]. Given a function  $f : \mathcal{X} \rightarrow \mathbb{R}$  whose gradient  $\nabla f$  exists almost everywhere on  $\mathcal{X}$ , the EGOP matrix  $\mathbf{C}_f \in \mathbb{R}^{d \times d}$  is defined by

$$\mathbf{C}_f := \mathbb{E}_X[\nabla f(X)\nabla f(X)^\top] = \int_{\mathcal{X}} \nabla f(\mathbf{x})\nabla f(\mathbf{x})^\top \rho(\mathbf{x}) d\mathbf{x}, \quad (11)$$

where  $\rho$  is a probability density function defined over  $\mathcal{X}$ . For technical convenience, throughout the paper we assume that  $\rho$  is strictly positive, i.e.,  $\rho(\mathbf{x}) > 0$  for all  $\mathbf{x} \in \mathcal{X}$ .

An eigendecomposition of the EGOP reveals directions in which the function has large (or small) variation on average. To see this, suppose  $\mathbf{v}$  is a unit-norm eigenvector of  $\mathbf{C}_f$  with eigenvalue  $\lambda$ . Then observe that

$$\lambda = \mathbf{v}^\top \mathbf{C}_f \mathbf{v} = \int_{\mathcal{X}} (\mathbf{v}^\top \nabla f(\mathbf{x}))^2 \rho(\mathbf{x}) = \|\partial_{\mathbf{v}} f\|_{L^2(\rho)}^2,$$

where  $\partial_{\mathbf{v}} f := \mathbf{v}^\top \nabla f$  denotes the directional derivative of  $f$  in the direction of  $\mathbf{v}$ . This shows that eigenvectors of  $\mathbf{C}_f$  with large eigenvalues correspond to directions for which the directional derivative of  $f$  is large in a  $L^2(\rho)$ -norm sense. On the other hand, eigenvectors with zero eigenvalue correspond to directions for which the directional derivative of  $f$  vanishes almost everywhere on  $\mathcal{X}$ , which implies  $f$  is constant in these directions, i.e.,  $f(\mathbf{x}) = f(\mathbf{x} + \sigma \mathbf{v})$  for almost all  $\mathbf{x} \in \mathcal{X}$  and  $\sigma \in \mathbb{R}$ . In particular, if the EGOP  $\mathbf{C}_f$  is low-rank, this implies  $f$  is constant in directions orthogonal to a low-dimensional subspace. This observation motivates the following definition:

**Definition 1** (Index rank). *We define the index rank of a function, denoted  $\text{rank}_I(f)$ , as the rank of its EGOP matrix  $\mathbf{C}_f$ .*

Additionally, we use the term *principal subspace* to refer to the range of  $\mathbf{C}_f$ , which coincides with the span of eigenvectors of  $\mathbf{C}_f$  associated with non-zero eigenvalues. Therefore, the index rank of a function coincides with the dimension of its principal subspace.

Our definition of index rank is closely related to multi-index models (1). To see this, note that if  $f : \mathcal{X} \rightarrow \mathbb{R}$  is a multi-index model of the form  $f(\mathbf{x}) = g(\mathbf{V}^\top \mathbf{x})$ , then  $\nabla f(\mathbf{x}) = \mathbf{V} \nabla g(\mathbf{V}^\top \mathbf{x})$  and so

$$\mathbf{C}_f = \mathbf{V} \mathbb{E}_X \left[ \nabla g(\mathbf{V}^\top X) \nabla g(\mathbf{V}^\top X)^\top \right] \mathbf{V}^\top. \quad (12)$$

This implies that the principal subspace of  $f$  will lie within its central subspace, and will be equal to the central subspace if  $\mathbb{E}_X \left[ \nabla g(\mathbf{V}^\top X) \nabla g(\mathbf{V}^\top X)^\top \right]$  is full rank.

We note that the index rank is distinct from other notions of nonlinear function rank proposed by Jacot in [22, 23]. Specifically, Jacot defines the *Jacobian rank* as  $\max_{\mathbf{x}} \text{rank}(Jf(\mathbf{x}))$  where  $Jf$  is the Jacobian of  $f$  and the *bottleneck rank* as the smallest integer  $k$  such that  $f$  can be factorized as  $f = h \circ g$  with inner dimension  $k$  where  $h$  and  $g$  are continuous and piecewise linear. These notions of nonlinear rank are connected to deep ReLU network representation costs. All three notions of rank (index, Jacobian, and bottleneck) capture different kinds of nonlinear low-dimensional structure. Notably, both the Jacobian and bottleneck ranks require that any function  $f$  mapping to a scalar must be rank-1, regardless of any latent structure in  $f$ , and so only vector-valued functions can have rank greater than 1. In contrast, our definition assigns scalar-valued functions different ranks



depending on the dimension of its principal subspace. We also discuss the extension of index rank to vector-valued functions in Appendix C.

Additionally, we note that learning an index-rank- $r$  function can be very different from the common practice of first reducing the dimension of the training features by projecting them onto the top  $r$  principal components of the training features and then feeding the reduced-dimension features into a neural network; that is, the principal subspace of the EGOP may be quite different from the features’ PCA subspace. Furthermore, as we detail in later sections, assuming the data is generated according to a multi-index model, the representation cost associated with adding linear layers promotes learning low-index-rank functions whose principal EGOP subspace is aligned with the central subspace; this is illustrated in Figure 2.

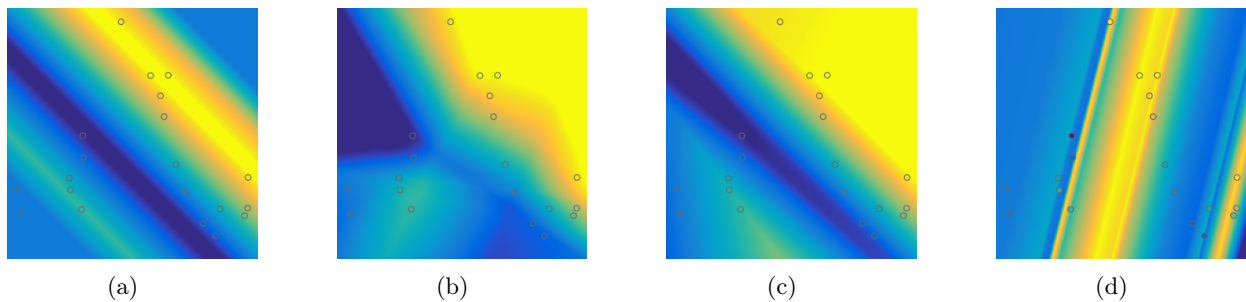


Figure 2: **Illustration of learning a low-index-rank function.** (a) Heatmap of a rank-1 data generating function  $f : \mathbb{R}^2 \rightarrow \mathbb{R}$  and locations of training samples. (b) Interpolant learned with  $L = 2$  layers, which does not exhibit rank-1 structure. (c) Interpolant learned with  $L = 4$  layers, which closely approximates the index-rank-1 structure of the data-generating function. (d) Result of performing PCA on training features to reduce their dimension to one, followed by learning with  $L = 2$  layers. This illustration highlights how the addition of linear layers promotes learning single-index models with a central subspace that may differ significantly from the features’ PCA subspace.

### 3.2 Mixed variation of a function

Performing an eigendecomposition on  $\mathbf{C}_f$  and discarding small eigenvalues yields an eigenbasis for a low-dimensional subspace that captures directions along which  $f$  has large variation. If the columns of a matrix  $\mathbf{V} \in \mathbb{R}^{d \times r}$  represent this eigenbasis, then  $f(\mathbf{x}) \approx f(\mathbf{x} + \mathbf{u})$  for all  $\mathbf{x} \in \mathcal{X}$  and all  $\mathbf{u} \in \text{range}(\mathbf{V})^\perp$ . Such functions are “approximately low-index-rank”. In this section, we introduce a notion of *mixed variation* to formalize and quantify this idea.

*Mixed variation function spaces* are informally defined in [64] to contain functions that are more regular in some directions than in others, and Parhi and Nowak [65] provide examples of neural networks adapting to a type of mixed variation. In this paper, we formally define the mixed variation of a function as follows:

**Definition 2** (Mixed variation). *For any  $q > 0$ , define the order  $q$  mixed variation of  $f$  to be the Schatten- $q$  (quasi-)norm of the matrix square-root of the EGOP:*

$$\mathcal{M}\mathcal{V}(f, q) := \|\mathbf{C}_f^{1/2}\|_{S^q} \tag{13}$$

Note that by defining the mixed variation in terms of the square root of the EGOP matrix we ensure the mixed variation is a 1-homogenous functional, i.e.,  $\mathcal{M}\mathcal{V}(\alpha f, q) = |\alpha| \mathcal{M}\mathcal{V}(f, q)$  for

all  $\alpha \in \mathbb{R}$ . Also, since for any matrix  $\mathbf{M}$  we have  $\|\mathbf{M}\|_{S^q}^q \rightarrow \text{rank}(\mathbf{M})$  as  $q \rightarrow 0$ , we see that  $\mathcal{M}\mathcal{V}(f, q)^q \rightarrow \text{rank}_I(f)$  as  $q \rightarrow 0$ .

As illustrated in Figure 3, functions may be full-index-rank according to Definition 1 but still have small mixed variation when they are “close” to having lower rank because they vary significantly more in one direction than another, consistent with the notions from [64, 65].

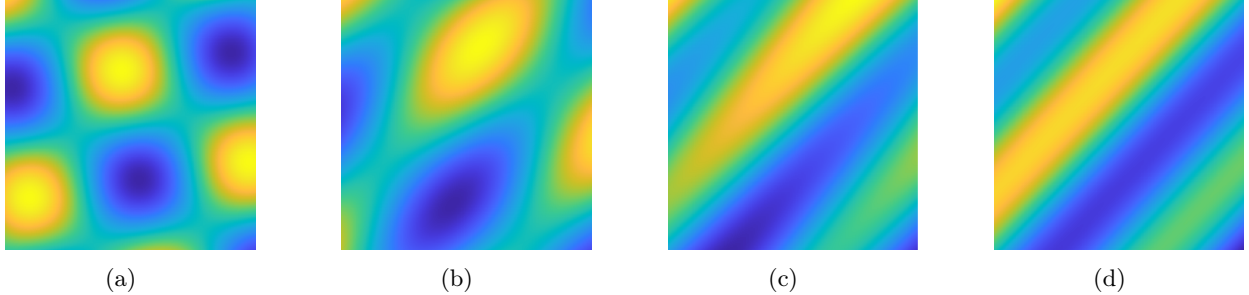


Figure 3: **Illustration of four functions  $f : \mathbb{R}^2 \rightarrow \mathbb{R}$  with mixed variation (Definition 2) decreasing from left to right.** All four functions are index rank 2 according to Definition 1, but the functions on the right with smaller mixed variation are closer to being index rank 1 because they vary significantly more in one direction than another.

## 4 The inductive bias of the $R_L$ cost

In this section, we show that minimizing the  $R_L$  cost promotes learning functions that are nearly low-index-rank and are “smooth” along their principal subspace. Specifically, Theorem 1 highlights how the relative importance of low dimensional structure versus smoothness changes with the number of linear layers. Thus, the number of linear layers in a model should be treated as a tunable hyperparameter at training time. In Corollaries 1 and 2 we further analyze how the  $R_L$  cost increasingly prioritizes low-rank structure as  $L$  increases. In Theorem 2 we provide bounds on the effective index rank of networks trained by minimizing the  $R_L$  cost. Omitted proofs of the results in this section can be found in Appendix B.

### 4.1 Index rank, mixed variation, and the $R_L$ cost

We begin by establishing a theorem that relates the  $R_L$  cost of a function  $f$  to its index rank, mixed variation, and  $R_2$  cost. This theorem underscores that low-rank structure and smoothness both influence the  $R_L$  cost, but their relative importance depends on  $L$ . In this context, we measure low-rank structure by the index rank or mixed variation of a function, and we measure smoothness via the  $R_2$  cost.

**Theorem 1.** *Let  $f \in \mathcal{N}_2(\mathcal{X})$  and  $L \geq 2$ . Then*

$$\max \left( \mathcal{M}\mathcal{V} \left( f, \frac{2}{L-1} \right)^{2/L}, R_2(f)^{2/L} \right) \leq R_L(f) \leq \text{rank}_I(f)^{\frac{L-2}{L}} R_2(f)^{2/L}.$$

The proof of this theorem can be found in Appendix B.2.

The upper bound tells us that a function  $f$  with both low index rank and low  $R_2$  cost will have a low  $R_L$  cost. Consider methods that explicitly learn a single-index or multi-index model to fit training data [47, 66, 40, 39, 43, 49, 45, 46]; such methods, by construction, ensure that  $f$  has low index rank and has a smooth link function. Thus Theorem 1 shows that such methods also control the  $R_L$  cost of their learned functions. Furthermore, the lower bound guarantees that if we minimize the  $R_L$  cost during training, then the corresponding  $R_2$  cost and mixed variation cannot be too high. That is,  $R_L$  minimizers will be smooth in the  $R_2$  sense, and will have low mixed variation.

Observe that the relative importance of the  $R_2$  cost and the index rank or mixed variation in the bounds above changes with  $L$ : as  $L$  increases, the terms  $\mathcal{M}\mathcal{V}(f, \frac{2}{L-1})^{2/L}$  and  $\text{rank}_I(f)^{(L-2)/L}$  both tend towards  $\text{rank}_I(f)$ , while  $R_2^{2/L}$  tends to one. This suggests that low-index-rank structure greatly influences the  $R_L$  cost as  $L$  increases. In fact, taking the limit as  $L$  tends to infinity, we have the following direct corollary of Theorem 1:

**Corollary 1.** *Let  $f \in \mathcal{N}_2(\mathcal{X})$ . Then*

$$\lim_{L \rightarrow \infty} R_L(f) = \text{rank}_I(f). \quad (14)$$

Even without taking limits, given a low-index-rank function and a high-index-rank function, for large enough  $L$  the low index rank function will have lower  $R_L$  cost. This idea is formalized in the following corollary of Theorem 1.

**Corollary 2.** *For all  $f_l, f_h \in \mathcal{N}_2(\mathcal{X})$  such that  $\text{rank}_I(f_l) < \text{rank}_I(f_h)$ , there is a value  $L_0$  such that  $L > L_0$  implies  $R_L(f_l) < R_L(f_h)$ .*

Note that Corollary 2 holds even when  $R_2(f_h) < R_2(f_l)$ . This has implications for interpolating  $R_L$ -cost minimizers. For example, suppose  $f_l$  and  $f_h$  both interpolate the training data, with  $\text{rank}_I(f_l) < \text{rank}_I(f_h)$ , but  $f_h$  is an  $R_2$ -minimizing interpolant. Then Corollary 2 implies there exists an  $L_0$  such that for all  $L \geq L_0$  we have  $R_L(f_h) > R_L(f_l)$ , which implies  $f_h$  cannot be an  $R_L$ -minimizing interpolant for all  $L \geq L_0$ . In the next subsection, we describe this effect more quantitatively by providing bounds on the (effective) index rank of interpolating  $R_L$ -cost minimizers.

## 4.2 Trained networks have low effective index rank

Theorem 1 has implications for the decay of the singular values of EGOP of trained networks, and thus for their *effective* index rank. In this section, we focus on networks that interpolate the data and minimize the  $R_L$  cost, but generalize to other idealized learning rules based on finding (near-)global minimizers in Appendix D.

To simplify the statement of our results, we first define the *singular values of a function*  $f : \mathcal{X} \rightarrow \mathbb{R}$ , as  $\sigma_k(f) = \sigma_k(\mathbf{C}_f^{1/2})$  for all  $k \in [d]$ , i.e., we identify the singular values of a function with the singular values of the (square root) of its EGOP. Note that the index rank of  $f$  is the number of non-zero singular values of  $f$ , while the order  $q$  mixed variation of  $f$  is the  $\ell^q$  (quasi-)norm of the singular values of  $f$ . We also define the  $\varepsilon$ -effective index rank of  $f$  in terms of its singular values as follows:

**Definition 3** (Effective index rank). *Given a function  $f : \mathcal{X} \rightarrow \mathbb{R}$  and a threshold  $\varepsilon > 0$ , define the  $\varepsilon$ -effective index rank of  $f$ , denoted by  $\text{rank}_{I,\varepsilon}(f)$ , to be the number of singular values of  $f$  larger than  $\varepsilon$ . That is,*

$$\text{rank}_{I,\varepsilon}(f) := |\{k : \sigma_k(f) > \varepsilon\}|. \quad (15)$$

Below, we bound the effective index rank of minimum  $R_L$ -cost interpolating solutions, which applies even when the data is not generated by a low-index-rank function. To do so, we define the *interpolation cost* associated with a collection of training data:

**Definition 4** (Interpolation cost). *Given training data  $\mathcal{D} = \{(\mathbf{x}_i, y_i)\}_{i=1}^n$  and a rank cutoff  $s$ , define its rank- $s$  interpolation cost by*

$$\mathcal{I}_s(\mathcal{D}) = \min_{f \in \mathcal{N}_2(\mathcal{X})} R_2(f) \text{ s.t. } \text{rank}_I(f) \leq s, f(\mathbf{x}_i) = y_i \forall i \in [n]. \quad (16)$$

*i.e.,  $\mathcal{I}_s(\mathcal{D})$  is the minimum  $R_2$  cost needed to interpolate the data with a function of index rank at most  $s$ .*

Provided the training features  $\{\mathbf{x}_i\}_{i=1}^n$  are distinct, the interpolation cost  $\mathcal{I}_s(\mathcal{D})$  is always well-defined for all  $s \in [d]$ . This is because an interpolant of index-rank one always exists. See Section 4.2 for an example, and Appendix B.4 for proof of this claim.

Now we give our main theorem in this section, which shows that interpolants minimizing the  $R_L$  cost have effective index ranks that decay with  $L$ .

**Theorem 2** (Effective index ranks of minimal-cost interpolants.). *Assume that  $\hat{f}_L$  is an  $R_L$ -minimal interpolant of the training data  $\mathcal{D}$  for some  $L \geq 2$  (i.e.,  $\hat{f}_L$  is a minimizer of (10)). Then given any  $\varepsilon > 0$ , we have the following bound on the  $\varepsilon$ -effective index rank of  $\hat{f}_L$ :*

$$\text{rank}_{I,\varepsilon}(\hat{f}_L) \leq \min_{s \in [d]} \left\lceil s \left( \frac{\mathcal{I}_s(\mathcal{D})}{\varepsilon \sqrt{s}} \right)^{\frac{2}{L-1}} \right\rceil. \quad (17)$$

*Additionally, there exists an  $\varepsilon^* > 0$  independent of  $L$  such that for all  $0 < \varepsilon \leq \varepsilon^*$  we have  $\text{rank}_{I,\varepsilon}(\hat{f}_L) \geq 1$  for all  $L \geq 2$ .*

Generalizations of Theorem 2 to interpolating functions that are near minimizers of the  $R_L$  cost and to functions that minimize the  $R_L$ -regularized empirical risk (8) are given in Appendix D.

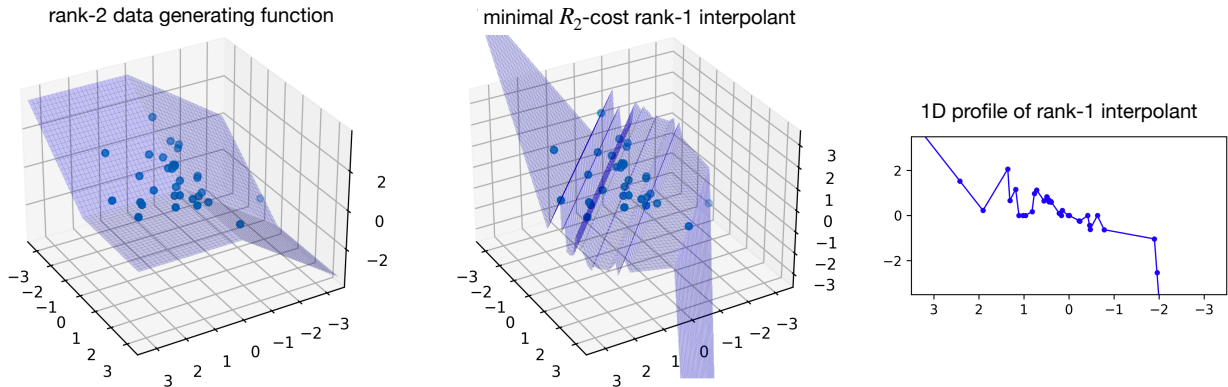


Figure 4: **Existence of rank deficient interpolants.** Left panel shows 32 training samples generated by the index-rank-2 function  $f^*(x_1, x_2) = [x_1]_+ - [x_2]_+$ , for which  $R_2(f^*) = 2$ . Middle panel shows  $f_1$ , the estimated minimal  $R_2$ -cost index-rank-one interpolant of the training samples, for which  $R_2(f_1) \approx 287.5$ . Right panel shows the 1D profile of the rank-one interpolant in the middle panel.

The bounds in Theorem 2 have several implications in the case that the data is generated by a function  $f^*$  that has index rank  $r$  and finite  $R_2$  cost. First, by considering the case  $s = r$  in the bound (17) and using the fact that  $\mathcal{I}_r(\mathcal{D}) \leq R_2(f^*)$ , we have the following direct corollary of Theorem 2:

**Corollary 3.** *Suppose the training data  $\mathcal{D}$  is generated by a function  $f^* \in \mathcal{N}_2(\mathcal{X})$  with  $\text{rank}_I(f^*) = r$ . Let  $\hat{f}_L$  be an  $R_L$ -minimal interpolant of the training data  $\mathcal{D}$ . Fix any  $\varepsilon > 0$ . Suppose  $L \geq 2$  is such that  $R_2(f^*) < \varepsilon\sqrt{r} \left(1 + \frac{1}{r}\right)^{\frac{L-1}{2}}$ . Then  $\text{rank}_{I,\varepsilon}(\hat{f}_L) \leq r$ .*

The above corollary shows that for sufficiently large  $L$ , any minimum  $R_L$ -cost interpolant always has effective index rank bounded above by the index rank of the data generating function, independent of the number of training samples. However, if the number of training samples is small, it is possible that an interpolant of index rank  $s < r$  and small  $R_2$  cost exists. In this case, the bounds in Theorem 2 imply  $\text{rank}_{I,\varepsilon}(\hat{f}_L) < r$  for sufficiently large  $L$ , i.e.,  $\hat{f}_L$  is rank deficient in the sense that its effective index rank is smaller than the index rank of the data generating function. In fact, Theorem 2 implies that for all sufficiently small values of  $\varepsilon$  there exists a sufficiently large  $L$  such that  $\text{rank}_{I,\varepsilon}(\hat{f}_L) = 1$ , regardless of the index rank of the data generating function.

Nevertheless, in our experiments training with standard gradient-based optimization techniques and using moderate values of  $L$  (e.g., between 3 and 9), we never observed rank-deficient models; see Section 5 for more details. Instead, we frequently observed that trained models had an effective index rank between the true rank of the task and the ambient dimension. Moreover, models trained with small amounts of label noise and a well-chosen depth  $L$  almost always had effective index ranks exactly equal to the true rank; see Figure 8 for illustration.

## 5 Numerical Experiments

To understand the practical consequences of the theoretical results in the previous section, we perform numerical experiments in which we train neural networks of the form (4) with varying values of  $L$  on simulated data where the ground truth is a low-index-rank function. More specifically, we create an index-rank- $r$  function  $f : \mathbb{R}^{20} \rightarrow \mathbb{R}$  by randomly generating  $\mathbf{a}, \mathbf{b} \in \mathbb{R}^{21}$  and a rank- $r$  matrix  $\mathbf{W} \in \mathbb{R}^{21 \times 20}$ . Under this setup, the function  $f(\mathbf{x}) = \mathbf{a}^\top [\mathbf{W}\mathbf{x} + \mathbf{b}]_+$  is an index-rank- $r$  function whose principal subspace is  $\text{range}(\mathbf{W}^\top)$  (or, one could also say that  $f$  is a single- or multi-index model with central subspace  $\text{range}(\mathbf{W}^\top)$ ). For  $r = 1$  and 2, we generate training datasets  $\{(\mathbf{x}_i, f(\mathbf{x}_i) + \sigma\varepsilon_i)\}_{i=1}^n$  of size  $n$  where  $\mathbf{x}_i \sim U\left[-\frac{1}{2}, \frac{1}{2}\right]^{20}$ ,  $\varepsilon_i \sim N(0, 1)$ , and the label noise standard deviation  $\sigma$  is either 0, 0.25, 0.5, or 1. For several different values of training samples  $n$ , we train neural networks of the form (4) by minimizing the  $\ell_2$ -regularized empirical risk (6) with a mean-squared error loss function  $\ell(z, y) = |z - y|^2$ . We tune the hyperparameters of depth ( $L$ ) and  $\ell_2$ -regularization strength ( $\lambda$ ) on a separate validation set. We compare against shallow ReLU networks without linear layers (i.e.,  $L = 2$ ) trained in the same way and with the hyperparameter  $\lambda$  tuned in the same way. See Appendix F for more training details.

We test the performance of the trained networks on  $m = 2048$  new test samples of the form  $(\mathbf{x}_i, f(\mathbf{x}_i) + \sigma\varepsilon_i)$  where either  $\mathbf{x}_i \sim U\left[-\frac{1}{2}, \frac{1}{2}\right]^{20}$  to measure in-distribution generalization (Figure 5) or  $\mathbf{x}_i \sim U\left[-1, 1\right]^{20}$  to measure out-of-distribution generalization (Figure 6). In Figures 5 and 6, we see that the regularization induced by adding linear layers helps improve in- and out-of-distribution generalization; models with linear layers approach the irreducible error of  $\sigma^2$  with fewer samples

than models without linear layers.<sup>2</sup>

Models trained with extra linear layers are better able to adapt to the multi-index model underlying the data because they have a low effective index rank. We estimate the EGOP singular values of the trained networks  $\hat{f}$  using the *average* gradient outer product (AGOP) matrix computed over the in-distribution test set:

$$\hat{\mathbf{C}}_{\hat{f}} := \frac{1}{m} \sum_{i=1}^m \nabla \hat{f}(\mathbf{x}_i) \nabla \hat{f}(\mathbf{x}_i)^\top. \quad (18)$$

As shown in [55], the AGOP is a good estimate of the EGOP with high probability. Thus, the singular values of  $\hat{f}$  can be well approximated by the singular values of the square root of the AGOP. The singular values for each model  $\hat{f}$  are shown in Figure 7. We observe that adding linear layers leads to trained networks with smaller singular values and lower effective index rank; the singular values  $\sigma_k$  for larger  $k$  of networks with extra linear layers are often many orders of magnitude smaller than their counterparts without linear layers.

We also see that models with linear layers generalize better because of improved alignment with the principal subspace of the ground truth function. We use the AGOP to estimate the alignment between the principal subspace of the trained model and the true central subspace of  $f$ . We measure the alignment between two  $r$ -dimensional subspaces  $\mathcal{U}, \mathcal{V}$  by their largest principal angle  $\angle(\mathcal{U}, \mathcal{V}) = \arcsin(\|\mathbf{P}_{\mathcal{U}} - \mathbf{P}_{\mathcal{V}}\|_{op})$ , where  $\mathbf{P}_{\mathcal{U}}$  and  $\mathbf{P}_{\mathcal{V}}$  denote the orthogonal projectors onto  $\mathcal{U}$  and  $\mathcal{V}$ , respectively [67]. In Figure 8 we show the largest principal angle between the principal subspace of  $f$  and the principal subspace of the trained models, estimated as the span of the top  $r$  eigenvectors of the AGOP. We also show the estimates of the effective index rank of the trained networks at the  $\varepsilon = 10^{-3}$  tolerance level. For models that have many singular values that are far from zero, including those trained without linear layers, the truncation to exactly  $r$  eigenvectors in computing the principal angle can give an overly generous estimate of the agreement between the learned principal subspace and principal subspace of the function used to generate the data. Even using this generous estimate, models with linear layers demonstrate better alignment.

## 6 Discussion, Limitations, and Future Directions

The representation cost expressions we derive offer new, quantitative insights into multi-layer networks trained using  $\ell_2$ -regularization. Specifically, we show that training a ReLU network with additional linear layers on the input side with  $\ell_2$ -regularization implicitly seeks a *low-dimensional* subspace such that after projecting the training data into this subspace it can be fit with a *smooth* function (in the sense of having a low two-layer representation cost). To characterize the representation cost in function space, we provide a formal definition of mixed variation (Definition 2) consistent with past usage [64, 13].

While we do not provide generalization bounds, our numerical experiments suggest that if low-index-rank structure is present in the data, adding linear layers results in an inductive bias that is helpful for generalization, particularly with small sample sizes when two-layer networks have larger generalization errors. An interesting direction for future work is to see if networks minimizing the multi-linear-layer representation cost can achieve generalization with fast rates (depending on the dimension of the latent central subspace) even in high-dimensional settings [43] and without constraining the network architecture (as in [47]) or training (as in [49]) to explicitly seek the central

---

<sup>2</sup>Because of the label noise, the expected squared-error of any model will be at least  $\sigma^2$ .

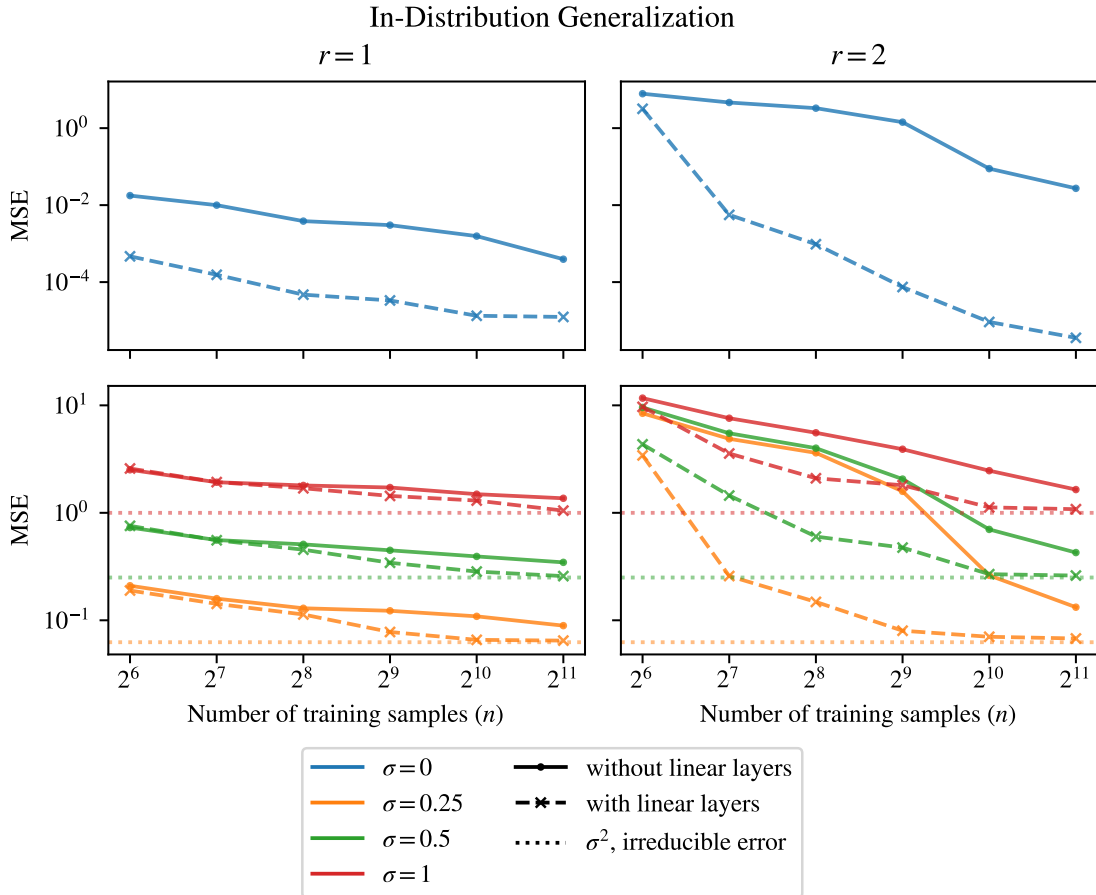


Figure 5: **Adding linear layers improves generalization on multi-index models.** In-distribution generalization performance of networks trained with or without extra linear layers on data from a single-index model (left) or multi-index model (right) with varying amounts of label noise. Models trained with extra linear layers demonstrate significantly improved generalization. (Bottom) Even in the presence of label noise, the generalization error of models with extra linear layers quickly approaches the irreducible error  $\sigma^2$  as the number of training samples ( $n$ ) increases.

subspace. An additional benefit of this ability to adapt to latent single- and multi-index structure is that networks with low-index-rank are inherently compressible [49].

It is important to note that the number of linear layers to add should be treated as a tunable hyperparameter; Theorem 2 implies that adding too many linear layers with a fixed number of training samples can result in global minimizers that underestimate the index rank of the ground truth function. However, the number of linear layers at which such rank-deficient solutions occur may be very large. In our experiments, we never observed rank-deficient solutions when training with a moderate number of linear layers ( $L \leq 9$ ), and using standard initialization schemes and optimization techniques.

One limitation of our theoretical analysis is the focus on properties of global or near-global minimizers. We do not analyze the dynamics of specific optimization algorithms, in contrast with [48], which provides generalization bounds in terms of sample complexity of a shallow network

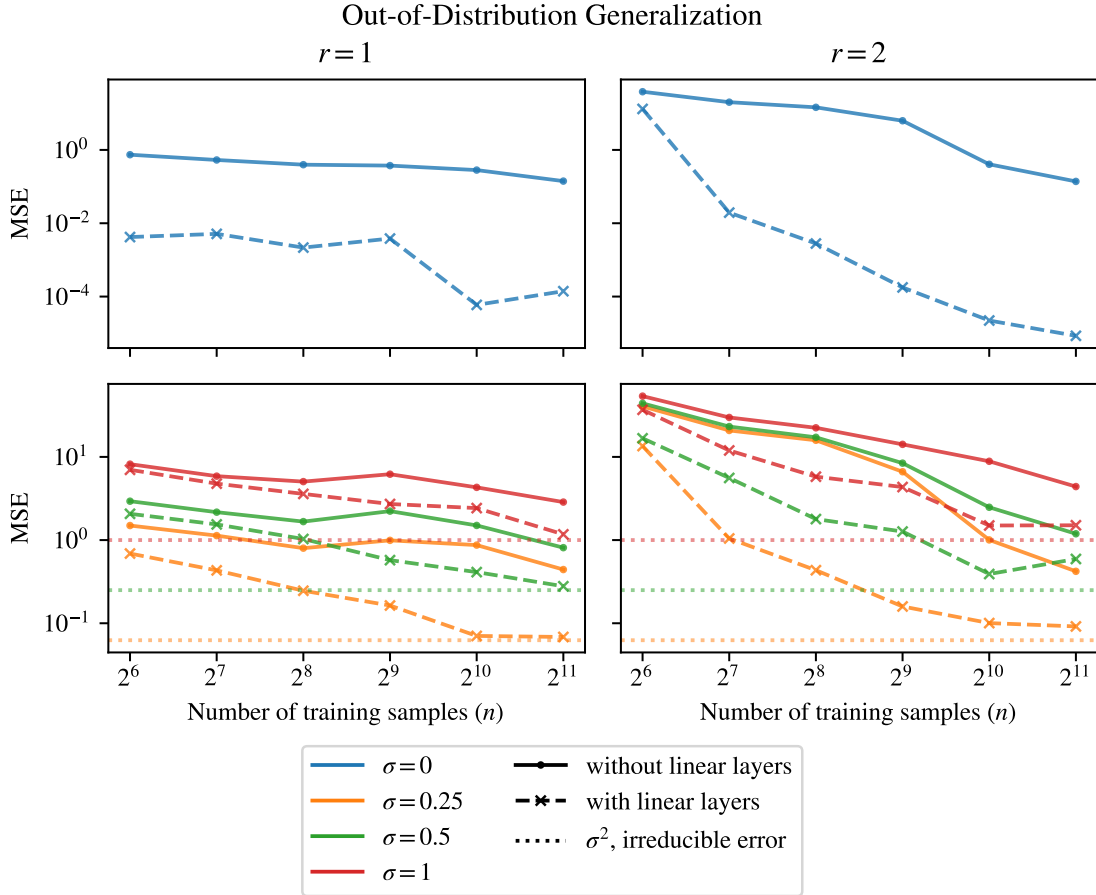


Figure 6: **Adding linear layers improves performance outside of the training distribution.** Out-of-distribution generalization performance of networks trained with or without extra linear layers on data from a single-index model (left) or multi-index model (right) with varying amounts of label noise.

trained with a modified form of gradient descent. An interesting extension of this work would be to analyze whether adding linear layers allows specific optimization algorithms to converge to functions with small  $R_L$  cost, as we observe in experiments. In that case, Theorem 2 suggests that these solutions would have small effective index rank.

Finally, a key limitation of the current work is that our analysis framework does not extend easily to deep networks with multiple nonlinear layers. Progress towards understanding this inductive bias is found in [22, 23], but more fully understanding the representation costs of general nonlinear deep networks remains a significant open problem for the community.

## Acknowledgements

R. Willett gratefully acknowledges the support of AFOSR grant FA9550-18-1-0166 and NSF grant DMS-2023109. G. Ongie was supported by NSF CRII award CCF-2153371. This material is based upon work supported by the NSF Graduate Research Fellowship under Grant No. DGE:2140001.



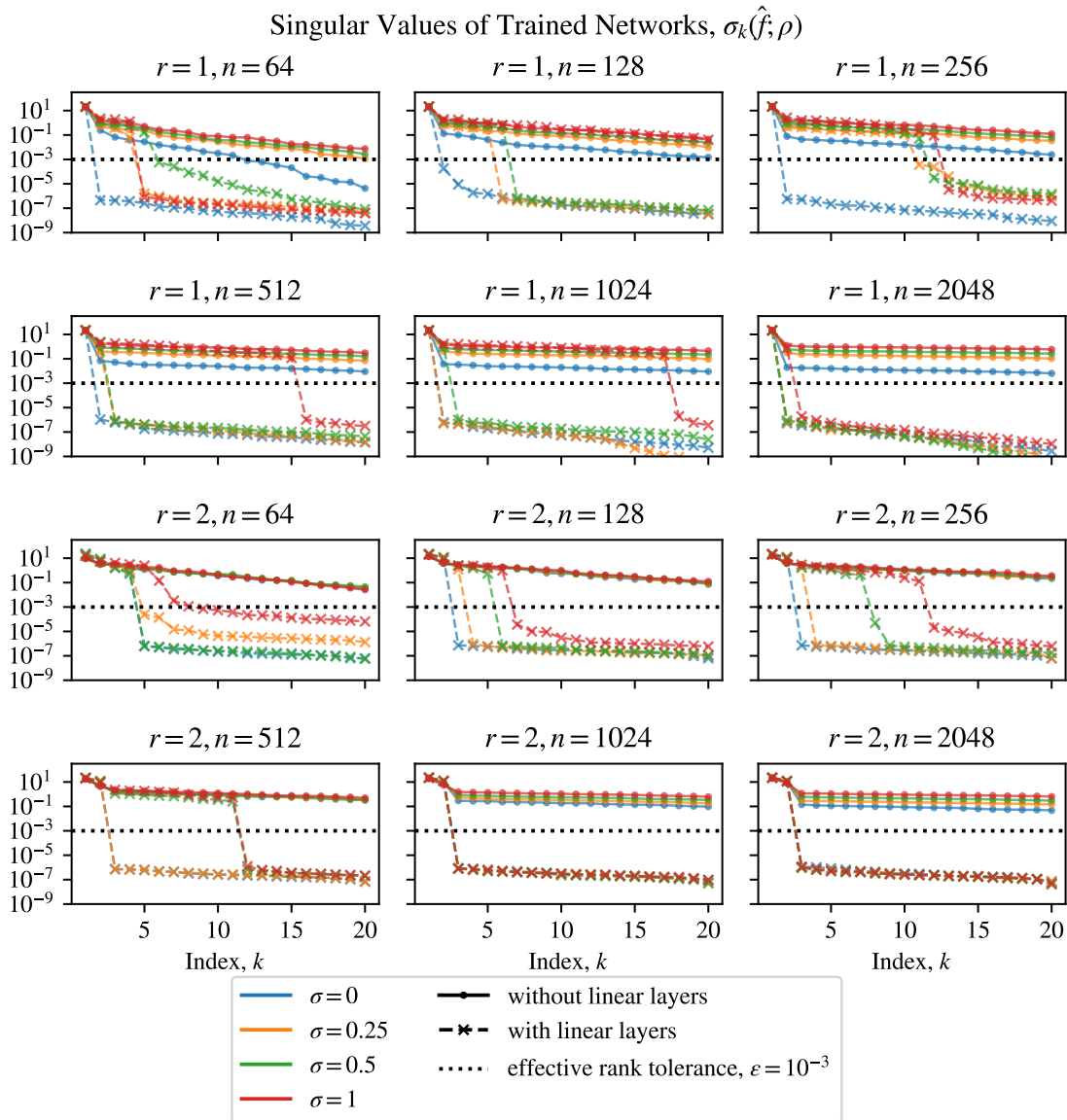


Figure 7: **Adding linear layers decreases the singular values of trained networks.** Singular values of trained networks trained with or without extra linear layers on data from a single-index model (left) or multi-index model (right) with varying amounts of label noise. Models with extra linear layers exhibit sharper singular value dropoff and have a smaller effective index rank at the  $\varepsilon = 10^{-3}$  tolerance level than models without linear layers.

## References

- [1] P. L. Bartlett, “For valid generalization the size of the weights is more important than the size of the network,” in *Advances in Neural Information Processing Systems*, pp. 134–140, 1997.
- [2] B. Neyshabur, R. Tomioka, and N. Srebro, “In search of the real inductive bias: On the role of implicit regularization in deep learning,” *arXiv preprint arXiv:1412.6614*, 2014.

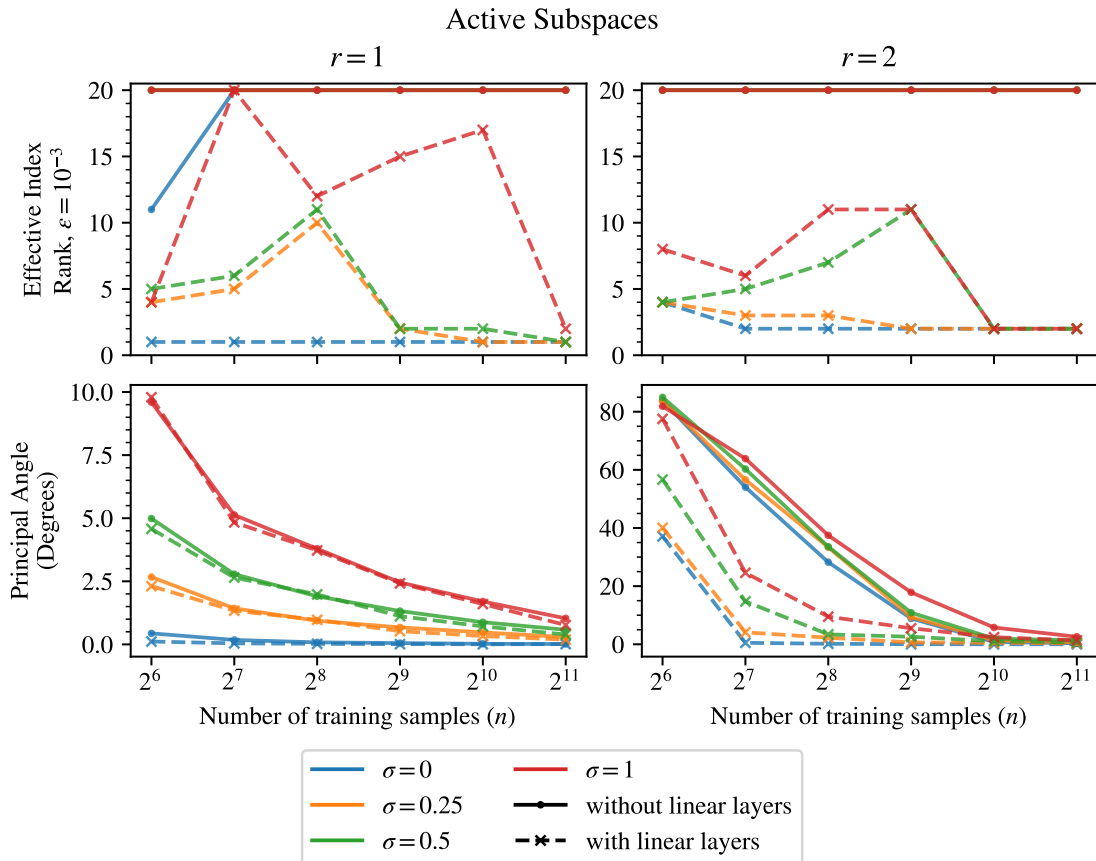


Figure 8: **Adding linear layers helps find networks with low effective index rank that are aligned with the true principal subspace.** Estimates of the effective index rank and principal subspace alignment of networks trained with or without extra linear layers on data from a single-index model (left) or multi-index model (right) with varying amounts of label noise. (Top) The effective index rank using a tolerance of  $\varepsilon = 10^{-3}$ . (Bottom) The largest principal angle between the principal subspace of  $f$  and the span of the top  $r$  eigenvectors of the AGOP of the trained model.

- [3] C. Zhang, S. Bengio, M. Hardt, B. Recht, and O. Vinyals, “Understanding deep learning (still) requires rethinking generalization,” *Communications of the ACM*, vol. 64, no. 3, pp. 107–115, 2021.
- [4] K. Lyu and J. Li, “Gradient descent maximizes the margin of homogeneous neural networks,” in *International Conference on Learning Representations*, 2020.
- [5] M. S. Nacson, S. Gunasekar, J. D. Lee, N. Srebro, and D. Soudry, “Lexicographic and depth-sensitive margins in homogeneous and non-homogeneous deep models,” *International Conference on Machine Learning*, 2019.
- [6] B. Neyshabur, R. Tomioka, and N. Srebro, “Norm-based capacity control in neural networks,” in *Conference on Learning Theory*, pp. 1376–1401, PMLR, 2015.
- [7] C. Wei, J. D. Lee, Q. Liu, and T. Ma, “Regularization matters: Generalization and optimization

- of neural nets vs their induced kernel,” *Advances in Neural Information Processing Systems*, vol. 32, 2019.
- [8] F. Bach, “Breaking the curse of dimensionality with convex neural networks,” *Journal of Machine Learning Research*, vol. 18, no. 19, pp. 1–53, 2017.
- [9] P. Savarese, I. Evron, D. Soudry, and N. Srebro, “How do infinite width bounded norm networks look in function space?,” in *Conference on Learning Theory*, pp. 2667–2690, 2019.
- [10] E. Boursier and N. Flammarion, “Penalising the biases in norm regularisation enforces sparsity,” *Advances in Neural Information Processing Systems*, vol. 36, pp. 57795–57824, 2023.
- [11] G. Ongie, R. Willett, D. Soudry, and N. Srebro, “A function space view of bounded norm infinite width ReLU nets: The multivariate case,” in *International Conference on Learning Representations*, 2020.
- [12] J. Shenouda, R. Parhi, K. Lee, and R. D. Nowak, “Vector-valued variation spaces and width bounds for DNNs: Insights on weight decay regularization,” *arXiv preprint arXiv:2305.16534*, 2023.
- [13] R. Parhi and R. D. Nowak, “Banach space representer theorems for neural networks and ridge splines,” *Journal of Machine Learning Research*, vol. 22, no. 43, pp. 1–40, 2021.
- [14] F. Bartolucci, E. De Vito, L. Rosasco, and S. Vigogna, “Understanding neural networks with reproducing kernel banach spaces,” *Applied and Computational Harmonic Analysis*, vol. 62, pp. 194–236, 2023.
- [15] M. Unser, “Ridges, neural networks, and the radon transform,” *Journal of Machine Learning Research*, vol. 24, no. 37, pp. 1–33, 2023.
- [16] M. Pilanci and T. Ergen, “Neural networks are convex regularizers: Exact polynomial-time convex optimization formulations for two-layer networks,” in *International Conference on Machine Learning*, pp. 7695–7705, PMLR, 2020.
- [17] T. Ergen and M. Pilanci, “Implicit convex regularizers of CNN architectures: Convex optimization of two-and three-layer networks in polynomial time,” in *International Conference on Learning Representations*, 2020.
- [18] T. Ergen and M. Pilanci, “Revealing the structure of deep neural networks via convex duality,” in *International Conference on Machine Learning*, pp. 3004–3014, PMLR, 2021.
- [19] R. Mulayoff, T. Michaeli, and D. Soudry, “The implicit bias of minima stability: A view from function space,” *Advances in Neural Information Processing Systems*, vol. 34, 2021.
- [20] M. S. Nacson, R. Mulayoff, G. Ongie, T. Michaeli, and D. Soudry, “The implicit bias of minima stability in multivariate shallow ReLU networks,” in *The Eleventh International Conference on Learning Representations*, 2022.
- [21] R. Parhi and R. D. Nowak, “What kinds of functions do deep neural networks learn? Insights from variational spline theory,” *SIAM Journal on Mathematics of Data Science*, vol. 4, no. 2, pp. 464–489, 2022.

- [22] A. Jacot, “Implicit bias of large depth networks: A notion of rank for nonlinear functions,” *International Conference on Learning Representations*, 2023.
- [23] A. Jacot, “Bottleneck structure in learned features: Low-dimension vs regularity tradeoff,” *Advances in Neural Information Processing Systems*, vol. 36, 2024.
- [24] Y. Wang, T. Ergen, and M. Pilanci, “Parallel deep neural networks have zero duality gap,” in *The Eleventh International Conference on Learning Representations*, 2022.
- [25] E. Zeger, Y. Wang, A. Mishkin, T. Ergen, E. Candès, and M. Pilanci, “A library of mirrors: Deep neural nets in low dimensions are convex lasso models with reflection features,” *arXiv preprint arXiv:2403.01046*, 2024.
- [26] T. Ergen and M. Pilanci, “Path regularization: A convexity and sparsity inducing regularization for parallel ReLU networks,” *Advances in Neural Information Processing Systems*, vol. 36, 2024.
- [27] S. Gunasekar, B. Woodworth, S. Bhojanapalli, B. Neyshabur, and N. Srebro, “Implicit regularization in matrix factorization,” in *2018 Information Theory and Applications Workshop (ITA)*, pp. 1–10, IEEE, 2018.
- [28] Z. Dai, M. Karzand, and N. Srebro, “Representation costs of linear neural networks: Analysis and design,” *Advances in Neural Information Processing Systems*, vol. 34, 2021.
- [29] Z. Ji and M. Telgarsky, “Gradient descent aligns the layers of deep linear networks,” in *International Conference on Learning Representations*, 2019.
- [30] A. Golubeva, G. Gur-Ari, and B. Neyshabur, “Are wider nets better given the same number of parameters?,” in *International Conference on Learning Representations*, 2021.
- [31] M. Khodak, N. A. Tenenholz, L. Mackey, and N. Fusi, “Initialization and regularization of factorized neural layers,” in *International Conference on Learning Representations*, 2020.
- [32] J. Ba and R. Caruana, “Do deep nets really need to be deep?,” in *Advances in Neural Information Processing Systems*, vol. 27, 2014.
- [33] G. Urban, K. J. Geras, S. E. Kahou, O. Aslan, S. Wang, A. Mohamed, M. Philipose, M. Richardson, and R. Caruana, “Do deep convolutional nets really need to be deep and convolutional?,” in *International Conference on Learning Representations*, 2016.
- [34] S. Arora, N. Cohen, and E. Hazan, “On the optimization of deep networks: Implicit acceleration by overparameterization,” in *International Conference on Machine Learning*, pp. 244–253, PMLR, 2018. <http://proceedings.mlr.press/v80/arora18a/arora18a.pdf>.
- [35] S. Arora, N. Cohen, W. Hu, and Y. Luo, “Implicit regularization in deep matrix factorization,” *Advances in Neural Information Processing Systems*, vol. 32, pp. 7413–7424, 2019.
- [36] N. Razin and N. Cohen, “Implicit regularization in deep learning may not be explainable by norms,” *Advances in Neural Information Processing Systems*, vol. 33, pp. 21174–21187, 2020.
- [37] N. Razin, A. Maman, and N. Cohen, “Implicit regularization in tensor factorization,” in *International Conference on Machine Learning*, pp. 8913–8924, 2021.

- [38] K. Zeng, C. E. Perez De Jesus, A. J. Fox, and M. D. Graham, “Autoencoders for discovering manifold dimension and coordinates in data from complex dynamical systems,” *Machine Learning: Science and Technology*, 2023.
- [39] R. Ganti, N. Rao, L. Balzano, R. Willett, and R. Nowak, “On learning high dimensional structured single index models,” in *Proceedings of the AAAI Conference on Artificial Intelligence*, vol. 31, 2017.
- [40] R. S. Ganti, L. Balzano, and R. Willett, “Matrix completion under monotonic single index models,” *Advances in Neural Information Processing Systems*, vol. 28, 2015.
- [41] A. Gollakota, P. Gopalan, A. Klivans, and K. Stavropoulos, “Agnostically learning single-index models using omnipredictors,” *Advances in Neural Information Processing Systems*, vol. 36, 2024.
- [42] S. M. Kakade, V. Kanade, O. Shamir, and A. Kalai, “Efficient learning of generalized linear and single index models with isotonic regression,” *Advances in Neural Information Processing Systems*, vol. 24, 2011.
- [43] H. Liu and W. Liao, “Learning functions varying along a central subspace,” *SIAM Journal on Mathematics of Data Science*, vol. 6, no. 2, pp. 343–371, 2024.
- [44] Y. Xia, “A multiple-index model and dimension reduction,” *Journal of the American Statistical Association*, vol. 103, no. 484, pp. 1631–1640, 2008.
- [45] X. Yin, B. Li, and R. D. Cook, “Successive direction extraction for estimating the central subspace in a multiple-index regression,” *Journal of Multivariate Analysis*, vol. 99, no. 8, pp. 1733–1757, 2008.
- [46] Y. Zhu and P. Zeng, “Fourier methods for estimating the central subspace and the central mean subspace in regression,” *Journal of the American Statistical Association*, vol. 101, no. 476, pp. 1638–1651, 2006.
- [47] A. Bietti, J. Bruna, C. Sanford, and M. J. Song, “Learning single-index models with shallow neural networks,” in *Advances in Neural Information Processing Systems*, 2022.
- [48] A. Damian, J. Lee, and M. Soltanolkotabi, “Neural networks can learn representations with gradient descent,” in *Conference on Learning Theory*, pp. 5413–5452, PMLR, 2022.
- [49] A. Mousavi-Hosseini, S. Park, M. Girotti, I. Mitliagkas, and M. A. Erdogdu, “Neural networks efficiently learn low-dimensional representations with SGD,” in *The Eleventh International Conference on Learning Representations*, 2022.
- [50] N. Ardeshir, D. J. Hsu, and C. H. Sanford, “Intrinsic dimensionality and generalization properties of the  $r$ -norm inductive bias,” in *The Thirty Sixth Annual Conference on Learning Theory*, pp. 3264–3303, PMLR, 2023.
- [51] M. Huh, H. Mobahi, R. Zhang, B. Cheung, P. Agrawal, and P. Isola, “The low-rank simplicity bias in deep networks,” *Transactions on Machine Learning Research*, 2022.

- [52] A. Radhakrishnan, D. Beaglehole, P. Pandit, and M. Belkin, “Mechanism for feature learning in neural networks and backpropagation-free machine learning models,” *Science*, vol. 383, no. 6690, pp. 1461–1467, 2024.
- [53] D. Beaglehole, P. Sůkeník, M. Mondelli, and M. Belkin, “Average gradient outer product as a mechanism for deep neural collapse,” *arXiv preprint arXiv:2402.13728*, 2024.
- [54] A. Radhakrishnan, M. Belkin, and D. Drusvyatskiy, “Linear recursive feature machines provably recover low-rank matrices,” *arXiv preprint arXiv:2401.04553*, 2024.
- [55] P. G. Constantine, *Active subspaces: Emerging ideas for dimension reduction in parameter studies*. SIAM, 2015.
- [56] P. G. Constantine, E. Dow, and Q. Wang, “Active subspace methods in theory and practice: Applications to kriging surfaces,” *SIAM Journal on Scientific Computing*, vol. 36, no. 4, pp. A1500–A1524, 2014.
- [57] A. M. Samarov, “Exploring regression structure using nonparametric functional estimation,” *Journal of the American Statistical Association*, vol. 88, no. 423, pp. 836–847, 1993.
- [58] M. Hristache, A. Juditsky, J. Polzehl, and V. Spokoiny, “Structure adaptive approach for dimension reduction,” *Annals of Statistics*, pp. 1537–1566, 2001.
- [59] Q. Wu, J. Guinney, M. Maggioni, and S. Mukherjee, “Learning gradients: predictive models that infer geometry and statistical dependence,” *The Journal of Machine Learning Research*, vol. 11, pp. 2175–2198, 2010.
- [60] S. Trivedi, J. Wang, S. Kpotufe, and G. Shakhnarovich, “A consistent estimator of the expected gradient outerproduct,” in *Conference on Uncertainty in Artificial Intelligence*, pp. 819–828, 2014.
- [61] G. Yuan, M. Xu, S. Kpotufe, and D. Hsu, “Efficient estimation of the central mean subspace via smoothed gradient outer products,” *arXiv preprint arXiv:2312.15469*, 2023.
- [62] S. Hanson and L. Pratt, “Comparing biases for minimal network construction with backpropagation,” *Advances in neural information processing systems*, vol. 1, pp. 177–185, 1988.
- [63] I. Loshchilov and F. Hutter, “Decoupled weight decay regularization,” in *International Conference on Learning Representations*, 2019.
- [64] D. L. Donoho, “High-dimensional data analysis: The curses and blessings of dimensionality,” *AMS Math Challenges Lecture*, vol. 1, no. 2000, p. 32, 2000.
- [65] R. Parhi and R. D. Nowak, “Near-minimax optimal estimation with shallow ReLU neural networks,” *IEEE Transactions on Information Theory*, 2022.
- [66] A. Cohen, I. Daubechies, R. DeVore, G. Kerkyacharian, and D. Picard, “Capturing ridge functions in high dimensions from point queries,” *Constructive Approximation*, vol. 35, pp. 225–243, 2012.

- [67] A. V. Knyazev and M. E. Argentati, “Principal angles between subspaces in an A-based scalar product: algorithms and perturbation estimates,” *SIAM Journal on Scientific Computing*, vol. 23, no. 6, pp. 2008–2040, 2002.
- [68] N. Srebro, J. Rennie, and T. Jaakkola, “Maximum-margin matrix factorization,” *Advances in Neural Information Processing Systems*, vol. 17, 2004.
- [69] F. Shang, Y. Liu, F. Shang, H. Liu, L. Kong, and L. Jiao, “A unified scalable equivalent formulation for Schatten quasi-norms,” *Mathematics*, vol. 8, no. 8, p. 1325, 2020.
- [70] B.-Y. Wang and B.-Y. Xi, “Some inequalities for singular values of matrix products,” *Linear algebra and its applications*, vol. 264, pp. 109–115, 1997.
- [71] L. C. Evans, *Partial differential equations*, vol. 19. American Mathematical Soc., 2nd ed., 2010.

# APPENDIX

## A Simplifying the representation cost

Our main result in this section is an explicit description of the  $R_L$  cost in terms of a penalty  $\Phi_L$  applied to the inner-layer weight  $\mathbf{W}$  matrix and outer-layer weight vector  $\mathbf{a}$  of a two-layer network, rather than the weights of an  $L$ -layer network.

First, we prove the general  $R_L$  cost can be re-cast as an optimization over two-layer networks, but where the cost associated with the inner-layer weight matrix  $\mathbf{W}$  changes with  $L$ :

**Lemma 1.** *Suppose  $f \in \mathcal{N}_2(\mathcal{X})$ . Then*

$$R_L(f) = \inf_{\theta \in \Theta_2} \frac{1}{L} \|\mathbf{a}\|_2^2 + \frac{L-1}{L} \|\mathbf{W}\|_{\mathcal{S}^q}^q \quad \text{s.t.} \quad f = h_\theta^{(2)}|_{\mathcal{X}} \quad (19)$$

where  $q := 2/(L-1)$  and  $\|\mathbf{W}\|_{\mathcal{S}^q}$  is the Schatten- $q$  quasi-norm, i.e., the  $\ell^q$  quasi-norm of the singular values of  $\mathbf{W}$ .

*Proof.* The result is a direct consequence of the following variational characterization of the Schatten- $q$  quasi-norm for  $q = 2/P$  where  $P$  is a positive integer:

$$\|\mathbf{W}\|_{\mathcal{S}^{2/P}}^{2/P} = \min_{\mathbf{W}=\mathbf{W}_1\mathbf{W}_2\cdots\mathbf{W}_P} \frac{1}{P} (\|\mathbf{W}_1\|_F^2 + \|\mathbf{W}_2\|_F^2 + \cdots + \|\mathbf{W}_P\|_F^2) \quad (20)$$

where the minimization is over all matrices  $\mathbf{W}_1, \dots, \mathbf{W}_P$  of compatible dimensions. The case  $P = 2$  is well-known (see, e.g., [68]). The general case for  $P \geq 3$  is established in [69, Corollary 3]. See also [24, Proposition 2].  $\square$

Part of the difficulty in interpreting the expression for the  $R_L$  cost in (19) is that it varies under different sets of parameters realizing the same function. In particular, consider the following rescaling of parameters: for any vector  $\boldsymbol{\lambda} \in \mathbb{R}^K$  with positive entries, by the 1-homogeneity of the ReLU activation we have

$$\mathbf{a}^\top [\mathbf{W}\mathbf{x} + \mathbf{b}]_+ + c = (\mathbf{D}_\lambda^{-1}\mathbf{a})^\top [\mathbf{D}_\lambda\mathbf{W}\mathbf{x} + \mathbf{D}_\lambda\mathbf{b}]_+ + c. \quad (21)$$

However, the value of the objective in (19) may vary between the two parameter sets realizing the same function. To account for this scaling invariance, we define a new loss function  $\Phi_L$  by optimizing over all such “diagonal” rescalings of units. Using the AM-GM inequality and a change of variables, one can prove that  $\Phi_L$  depends only on  $\mathbf{W}$  and  $\mathbf{a}$  only through the  $K \times d$  matrix  $\mathbf{D}_\mathbf{a}\mathbf{W}$ . This leads us to the following result.

**Lemma 2.** *For any  $f \in \mathcal{N}_2(\mathcal{X})$ , we have*

$$R_L(f) = \inf_{\theta \in \Theta_2} \Phi_L(\mathbf{D}_\mathbf{a}\mathbf{W}) \quad \text{s.t.} \quad f = h_\theta^{(2)}|_{\mathcal{X}}. \quad (22)$$

where the function  $\Phi_L$  given a matrix  $\mathbf{M}$  is defined as

$$\Phi_L(\mathbf{M}) = \inf_{\substack{\|\boldsymbol{\lambda}\|_2=1 \\ \lambda_k > 0, \forall k}} \|\mathbf{D}_\lambda^{-1}\mathbf{M}\|_{\mathcal{S}^{2/(L-1)}}^{2/L}. \quad (23)$$



*Proof.* Fix any parameterization  $f = h_\theta^{(2)}|_{\mathcal{X}}$  with  $\theta = (\mathbf{W}, \mathbf{a}, \mathbf{b}, c)$ . Without loss of generality, assume  $\mathbf{a}$  has all nonzero entries. By positive homogeneity of the ReLU, for any vector  $\boldsymbol{\lambda} \in \mathbb{R}^K$  with positive entries (which we denote by  $\boldsymbol{\lambda} > 0$ ) the rescaled parameters  $\theta' = (\mathbf{D}_\lambda^{-1}\mathbf{W}, \mathbf{D}_\lambda\mathbf{a}, \mathbf{D}_\lambda^{-1}\mathbf{b}, c)$  also satisfy  $f = h_{\theta'}^{(2)}|_{\mathcal{X}}$ . Therefore, by Lemma 1 we have

$$R_L(f) = \inf_{\theta \in \Theta_2} \frac{1}{L} \|\mathbf{a}\|_2^2 + \frac{L-1}{L} \|\mathbf{W}\|_{\mathcal{S}^{2/(L-1)}}^{2/(L-1)} \quad \text{s.t. } f = h_\theta^{(2)}|_{\mathcal{X}} \quad (24)$$

$$= \inf_{\theta \in \Theta_2} \inf_{\boldsymbol{\lambda} > 0} \frac{1}{L} \|\mathbf{D}_\lambda \mathbf{a}\|_2^2 + \frac{L-1}{L} \|\mathbf{D}_\lambda^{-1} \mathbf{W}\|_{\mathcal{S}^{2/(L-1)}}^{2/(L-1)} \quad \text{s.t. } f = h_\theta^{(2)}|_{\mathcal{X}}. \quad (25)$$

Additionally, for any fixed  $\boldsymbol{\lambda} > 0$ , we may separately minimize over all scalar multiples  $c\boldsymbol{\lambda}$  where  $c > 0$ , to get

$$\inf_{\boldsymbol{\lambda} > 0} \frac{1}{L} \|\mathbf{D}_\lambda \mathbf{a}\|_2^2 + \frac{L-1}{L} \|\mathbf{D}_\lambda^{-1} \mathbf{W}\|_{\mathcal{S}^{2/(L-1)}}^{2/(L-1)} \quad (26)$$

$$= \inf_{\boldsymbol{\lambda} > 0} \left( \inf_{c > 0} c^2 \frac{1}{L} \|\mathbf{D}_\lambda \mathbf{a}\|_2^2 + c^{-2/(L-1)} \frac{L-1}{L} \|\mathbf{D}_\lambda^{-1} \mathbf{W}\|_{\mathcal{S}^{2/(L-1)}}^{2/(L-1)} \right) \quad (27)$$

$$= \inf_{\boldsymbol{\lambda} > 0} \left( \|\mathbf{D}_\lambda \mathbf{a}\|_2 \|\mathbf{D}_\lambda^{-1} \mathbf{W}\|_{\mathcal{S}^{2/(L-1)}} \right)^{2/L} \quad (28)$$

where the final equality follows by the weighted AM-GM inequality: for all  $a, b > 0$ , it holds that  $\frac{1}{L}a + \frac{L-1}{L}b \geq (ab^{L-1})^{1/L}$ , which holds with equality when  $a = b$ . Here we have  $a = (c\|\mathbf{D}_\lambda \mathbf{a}\|_2)^2$  and  $b = (c^{-1}\|\mathbf{D}_\lambda^{-1} \mathbf{W}\|_{\mathcal{S}^{2/(L-1)}})^{2/(L-1)}$ , and there exists a  $c > 0$  for which  $a = b$ , hence we obtain the lower bound.

Finally, performing the invertible change of variables  $\boldsymbol{\lambda} \mapsto \boldsymbol{\lambda}'$  defined by  $\lambda'_k = |a_k| \lambda_k$  for all  $k = 1, \dots, K$ , we have

$$\inf_{\boldsymbol{\lambda} > 0} \left( \|\mathbf{D}_\lambda \mathbf{a}\|_2 \|\mathbf{D}_\lambda^{-1} \mathbf{W}\|_{\mathcal{S}^{2/(L-1)}} \right)^{2/L} = \inf_{\boldsymbol{\lambda}' > 0} \left( \|\boldsymbol{\lambda}'\|_2 \|\mathbf{D}_{\boldsymbol{\lambda}'}^{-1} \mathbf{D}_\mathbf{a} \mathbf{W}\|_{\mathcal{S}^{2/(L-1)}} \right)^{2/L} \quad (29)$$

$$= \inf_{\substack{\boldsymbol{\lambda}' > 0 \\ \|\boldsymbol{\lambda}'\|_2 = 1}} \|\mathbf{D}_{\boldsymbol{\lambda}'}^{-1} \mathbf{D}_\mathbf{a} \mathbf{W}\|_{\mathcal{S}^{2/(L-1)}}^{2/L} \quad (30)$$

where we are able to constrain  $\boldsymbol{\lambda}'$  to be unit norm since  $\|\boldsymbol{\lambda}'\|_2 \|\mathbf{D}_{\boldsymbol{\lambda}'}^{-1} \mathbf{D}_\mathbf{a} \mathbf{W}\|_{\mathcal{S}^{2/(L-1)}}$  is invariant to scaling  $\boldsymbol{\lambda}'$  by positive constants.  $\square$

In the case of  $L = 2$ , the infimum in (23) can be computed explicitly as  $\Phi_2(\mathbf{M}) = \sum_{k=1}^K \|\mathbf{m}_k\|_2$ , where  $\mathbf{m}_k$  is the  $k$ th row of  $\mathbf{M}$ . Notice that  $\Phi_2(\mathbf{D}_\mathbf{a} \mathbf{W}) = \sum_{k=1}^K |a_k| \|\mathbf{w}_k\|_2$ , which agrees with the expression in (9) after rescaling so that  $\|\mathbf{w}_k\|_2 = 1$  for all  $k$ .

When  $L > 2$ , we are unable to find a closed-form expression for  $\Phi_L$ . However, (23) still gives some insight into the kinds of functions that have small  $R_L$  costs. Note that Schatten- $q$  quasi-norms with  $0 < q \leq 1$  are often used as a surrogate for the rank penalty. Intuitively, the expression for  $\Phi_L$  reveals that functions with small  $R_L$  cost have a low-rank inner-layer weight matrix  $\mathbf{W}$  and a sparse outer-layer weight vector  $\mathbf{a}$ . This claim is formally strengthened in the following lemma.

**Lemma 3.** *For all  $L \geq 2$  and all matrices  $\mathbf{M}$ , we have*

$$\Phi_2(\mathbf{M})^{2/L} \leq \Phi_L(\mathbf{M}) \leq \text{rank}(\mathbf{M})^{(L-2)/L} \Phi_2(\mathbf{M})^{2/L}. \quad (31)$$

*Additionally,*

$$\|\mathbf{M}\|_{\mathcal{S}^{2/L}}^{2/L} \leq \Phi_L(\mathbf{M}) \quad (32)$$

*Proof.* First, we prove the string of inequalities in (31). Let  $q \in (0, 1]$  and  $\boldsymbol{\sigma} \in \mathbb{R}^n$  be a vector with non-negative entries. Since the function  $t \mapsto t^{2/q}$  is convex, we can use Jensen's inequality to see that

$$n^{-\frac{2}{q}} \|\boldsymbol{\sigma}\|_q^2 = \left( \frac{1}{n} \sum_{i=1}^n \sigma_i^q \right)^{\frac{2}{q}} \leq \frac{1}{n} \left( \sum_{i=1}^n \sigma_i^2 \right) = n^{-1} \|\boldsymbol{\sigma}\|_2^2. \quad (33)$$

Thus

$$\|\boldsymbol{\sigma}\|_2 \leq \|\boldsymbol{\sigma}\|_q \leq n^{\frac{1}{q} - \frac{1}{2}} \|\boldsymbol{\sigma}\|_2. \quad (34)$$

When  $q = \frac{2}{L-1}$ , we have  $\frac{1}{q} - \frac{1}{2} = \frac{L-2}{2}$ . Extending this result to Schatten norms and raising all expressions to the  $2/L$  power, we see that for any rank- $r$  matrix  $\mathbf{M}$ ,

$$\|\mathbf{M}\|_F^{2/L} \leq \|\mathbf{M}\|_{S^q}^{2/L} \leq r^{\frac{L-2}{L}} \|\mathbf{M}\|_F^{2/L}. \quad (35)$$

Therefore,

$$\Phi_2(\mathbf{M})^{2/L} \leq \Phi_L(\mathbf{M}) \leq (\text{rank } \mathbf{M})^{\frac{L-2}{L}} \Phi_2(\mathbf{M})^{2/L}. \quad (36)$$

Now we prove the inequality in (32). In [70] it is shown that given matrices  $\mathbf{A} \in \mathbb{R}^{d \times K}$ ,  $\mathbf{B} \in \mathbb{R}^{K \times K}$  and a constant  $q > 0$ ,

$$\|\mathbf{AB}\|_{S^q}^q = \sum_{k=1}^K \sigma_k^q(\mathbf{AB}) \geq \sum_{k=1}^K \sigma_k^q(\mathbf{B}) \sigma_{K-k+1}^q(\mathbf{A}). \quad (37)$$

We apply this result to  $\mathbf{D}_\lambda^{-1} \mathbf{M}$  where  $\lambda > 0$ :

$$\|\mathbf{D}_\lambda^{-1} \mathbf{M}\|_{S^{\frac{2}{L-1}}}^{\frac{2}{L-1}} \geq \sum_{k=1}^K \sigma_k^{\frac{2}{L-1}}(\mathbf{M}) \sigma_{K-k+1}^{\frac{2}{L-1}}(\mathbf{D}_\lambda^{-1}) \quad (38)$$

$$= \sum_{k=1}^K \sigma_k^{\frac{2}{L-1}}(\mathbf{M}) \sigma_k^{-\frac{2}{L-1}}(\mathbf{D}_\lambda). \quad (39)$$

Next, we take the infimum over both sides and replace  $\lambda$  with its ordered version,  $\boldsymbol{\mu}$ :

$$\Phi_L(\mathbf{M})^{\frac{L}{L-1}} \geq \inf_{\substack{\|\boldsymbol{\lambda}\|_2=1, \\ \lambda_k > 0, \forall k}} \sum_{k=1}^K \sigma_k^{\frac{2}{L-1}}(\mathbf{M}) \sigma_k^{-\frac{2}{L-1}}(\mathbf{D}_\lambda). \quad (40)$$

$$\geq \min_{\substack{\|\boldsymbol{\mu}\|_2=1, \\ \mu_1 \geq \mu_2 \geq \dots \geq \mu_K \geq 0}} \sum_{k=1}^K \sigma_k^{\frac{2}{L-1}}(\mathbf{M}) \mu_k^{-\frac{2}{L-1}} \quad (41)$$

Using Lagrange multipliers, we find that

$$\min_{\substack{\|\boldsymbol{\mu}\|_2=1, \\ \mu_1 \geq \mu_2 \geq \dots \geq \mu_K \geq 0}} \sum_{k=1}^K \sigma_k^{2/(L-1)}(\mathbf{M}) \mu_k^{-2/(L-1)} = \|\mathbf{M}\|_{S^{2/L}}^{2/(L-1)} \quad (42)$$

Therefore,

$$\Phi_L(\mathbf{M}) \geq \|\mathbf{M}\|_{S^{2/L}}^{2/L}. \quad (43)$$

□

Since both the upper bound from (31) and the lower bound from (32) tend toward the rank of  $\mathbf{M}$  as  $L$  goes to infinity, so does  $\Phi_L$ .

## B Proofs and Technical Details for Results in Section 4

### B.1 Index Ranks of Neural Networks

Observe that if  $f(\mathbf{x}) = a[\mathbf{w}^\top \mathbf{x} + b]_+$  then  $\nabla f(\mathbf{x}) = aU(\mathbf{w}^\top \mathbf{x} + b)\mathbf{w}$  for almost all  $\mathbf{x} \in \mathcal{X}$  where  $U$  is the unit step function. This implies that  $\nabla f(\mathbf{x})\nabla f(\mathbf{x})^\top = a^2U(\mathbf{w}^\top \mathbf{x} + b)\mathbf{w}\mathbf{w}^\top$ . Likewise, if  $f \in \mathcal{N}_2(\mathcal{X})$  and  $f = h_\theta^{(2)}|_{\mathcal{X}}$  for some  $\theta = (\mathbf{W}, \mathbf{a}, \mathbf{b}, c)$ , then for almost all  $\mathbf{x} \in \mathcal{X}$ ,

$$\nabla f(\mathbf{x})\nabla f(\mathbf{x})^\top = \sum_{k=1}^K \sum_{j=1}^K a_k a_j U(\mathbf{w}_k^\top \mathbf{x} + b_k) U(\mathbf{w}_j^\top \mathbf{x} + b_j) \mathbf{w}_k \mathbf{w}_j^\top = (\mathbf{D}_a \mathbf{W})^\top \mathbf{U}_\theta(\mathbf{x}) \mathbf{D}_a \mathbf{W} \quad (44)$$

where  $\mathbf{U}_\theta(\mathbf{x})$  is the matrix of unit co-activations at  $\mathbf{x}$ . That is, the entries of  $\mathbf{U}_\theta(\mathbf{x})$  are of the form  $U(\mathbf{w}_k^\top \mathbf{x} + b_k)U(\mathbf{w}_j^\top \mathbf{x} + b_j)$  and so will be one if and only if both unit  $k$  and unit  $j$  are active at  $\mathbf{x}$ . Taking expectations gives

$$\mathbf{C}_f = (\mathbf{D}_a \mathbf{W})^\top \mathbb{E}_X[\mathbf{U}_\theta(X)] \mathbf{D}_a \mathbf{W}. \quad (45)$$

The expression above for  $\mathbf{C}_f$  allows us to connect  $\text{rank}_I(f)$  to  $\text{rank}(\mathbf{D}_a \mathbf{W})$ . We use the following technical lemma, proved in the Appendix E.1.

**Lemma 4.** *Assume  $\mathcal{X}$  is convex and has nonempty interior. Let  $f \in \mathcal{N}_2(\mathcal{X})$  and let  $\nabla f$  denote its weak gradient. Let  $\mathbf{u} \in \mathbb{R}^d$ . If  $\nabla f(\mathbf{x})^\top \mathbf{u} = 0$  for almost all  $\mathbf{x} \in \mathcal{X}$ , then  $f(\mathbf{x} + \mathbf{u}) = f(\mathbf{x})$  for all  $\mathbf{x} \in \mathcal{X}$  such that  $\mathbf{x} + \mathbf{u} \in \mathcal{X}$ .*

This lemma allows us to take the infimum in (22) over parameterizations of  $f$  with the same rank as  $f$ , as stated in the next lemma.

**Lemma 5.** *Assume  $\mathcal{X} \subseteq \mathbb{R}^d$  is either a bounded convex set with nonempty interior or else  $\mathcal{X} = \mathbb{R}^d$ . Let  $f \in \mathcal{N}_2(\mathcal{X})$ . Then*

$$R_L(f) = \inf_{\theta \in \Theta_2} \Phi_L(\mathbf{D}_a \mathbf{W}) \quad \text{s.t.} \quad f = h_\theta^{(2)}|_{\mathcal{X}} \quad \text{and} \quad \text{rank}_I(f) = \text{rank}(\mathbf{D}_a \mathbf{W}). \quad (46)$$

*Proof.* By (45), any parameterization  $\theta = (\mathbf{W}, \mathbf{a}, \mathbf{b}, c) \in \Theta_2$  of  $f$  satisfies  $\text{rank}_I(f) \leq \text{rank}(\mathbf{D}_a \mathbf{W})$ . It suffices to show that for all  $\theta = (\mathbf{W}, \mathbf{a}, \mathbf{b}, c) \in \Theta_2$  such that  $f = h_\theta^{(2)}|_{\mathcal{X}}$ , there is some  $\theta' = (\mathbf{W}', \mathbf{a}', \mathbf{b}', c') \in \Theta_2$  such that  $f = h_{\theta'}^{(2)}|_{\mathcal{X}}$ ,  $\text{rank}_I(f) \geq \text{rank}(\mathbf{D}_{\mathbf{a}'} \mathbf{W}')$ , and  $\Phi_L(\mathbf{D}_{\mathbf{a}'} \mathbf{W}') \leq \Phi_L(\mathbf{D}_a \mathbf{W})$ .

Fix a parameterization  $\theta = (\mathbf{W}, \mathbf{a}, \mathbf{b}, c)$  of  $f$  so that  $f = h_\theta^{(2)}|_{\mathcal{X}}$ . Let  $\mathbf{P}$  denote the orthogonal projector onto the range of  $\mathbf{C}_f$ . If  $\mathcal{X} = \mathbb{R}^d$ , then choosing  $\theta' = (\mathbf{W}\mathbf{P}, \mathbf{a}, \mathbf{b}, c)$  suffices; for any  $\mathbf{x} \in \mathbb{R}^d$ , we have

$$h_{\theta'}^{(2)}(\mathbf{x}) = h_\theta^{(2)}(\mathbf{P}\mathbf{x}) = f(\mathbf{P}\mathbf{x}) = f(\mathbf{x}) \quad (47)$$

because Lemma 4 implies that  $f$  is constant along the nullspace of  $\mathbf{C}_f$ . Additionally, notice that  $\text{rank}_I(f) = \text{rank}(\mathbf{P}) \geq \text{rank}(\mathbf{D}_a \mathbf{W}\mathbf{P})$ . Finally, because multiplying by a projection matrix can only decrease singular values, we get  $\Phi_L(\mathbf{D}_a \mathbf{W}) \geq \Phi_L(\mathbf{D}_a \mathbf{W}\mathbf{P})$ . If  $\mathcal{X}$  is a bounded convex set, the choice of  $\theta'$  becomes more delicate; see Appendix E.2 for the full proof.  $\square$

## B.2 Proof of Theorem 1

*Proof.* Let  $f \in \mathcal{N}_2(\mathcal{X})$  and  $L \geq 2$ . From the characterization of  $R_L$  in terms of  $\Phi_L$  from Lemma 2 and the bounds on  $\Phi_L$  from Lemma 3, we get

$$R_2(f)^{2/L} \leq R_L(f) \leq \inf_{\theta: f=h_\theta^{(2)}|_{\mathcal{X}}} \text{rank}(\mathbf{D}_a \mathbf{W})^{(L-2)/L} \Phi_2(\mathbf{D}_a \mathbf{W})^{2/L}. \quad (48)$$

By Lemma 5, the characterization of  $R_L$  in terms of  $\Phi_L$  can be considered over just those parameterizations of  $f$  where  $\text{rank}(\mathbf{D}_a \mathbf{W})$  matches  $\text{rank}_I(f)$ . This allows us to upper bound the right-hand side in (48) as follows:

$$\text{rank}_I(f)^{(L-2)/L} R_2(f)^{2/L} \quad (49)$$

$$= \text{rank}_I(f)^{(L-2)/L} \inf_{\substack{\theta: f=h_\theta^{(2)}|_{\mathcal{X}} \\ \text{rank}_I(f)=\text{rank}(\mathbf{D}_a \mathbf{W})}} \Phi_2(\mathbf{D}_a \mathbf{W})^{2/L} \quad (50)$$

$$= \inf_{\substack{\theta: f=h_\theta^{(2)}|_{\mathcal{X}} \\ \text{rank}_I(f)=\text{rank}(\mathbf{D}_a \mathbf{W})}} \text{rank}(\mathbf{D}_a \mathbf{W})^{(L-2)/L} \Phi_2(\mathbf{D}_a \mathbf{W})^{2/L} \quad (51)$$

$$\geq \inf_{\theta: f=h_\theta^{(2)}|_{\mathcal{X}}} \text{rank}(\mathbf{D}_a \mathbf{W})^{(L-2)/L} \Phi_2(\mathbf{D}_a \mathbf{W})^{2/L}. \quad (52)$$

Therefore

$$R_L(f) \leq \text{rank}_I(f)^{(L-2)/L} R_2(f)^{2/L}. \quad (53)$$

Now we prove

$$\mathcal{M}\mathcal{V}\left(f, \frac{2}{L-1}\right)^{2/L} \leq R_L(f). \quad (54)$$

Assume  $f = h_\theta^{(2)}|_{\mathcal{X}}$  for some  $\theta = (\mathbf{W}, \mathbf{a}, \mathbf{b}, c)$ . Let  $\mathbb{E}_X[\mathbf{U}_\theta(X)]^{1/2}$  be a matrix square root of  $\mathbb{E}_X[\mathbf{U}_\theta(X)]$ . By (45), a nonsymmetric square root of  $\mathbf{C}_f$  is given by  $\mathbf{C}_f^{1/2} = \mathbb{E}_X[\mathbf{U}_\theta(X)]^{1/2} \mathbf{D}_a \mathbf{W}$ , and so we have  $\mathcal{M}\mathcal{V}(f, q) = \|\mathbb{E}_X[\mathbf{U}_\theta(X)]^{1/2} \mathbf{D}_a \mathbf{W}\|_{S^q}$ . Fix any vector  $\boldsymbol{\lambda} > 0$  such that  $\|\boldsymbol{\lambda}\|_2 = 1$ . Then we have

$$\mathcal{M}\mathcal{V}(f, q) = \|\mathbb{E}_X[\mathbf{U}_\theta(X)]^{1/2} \mathbf{D}_a \mathbf{W}\|_{S^q} \quad (55)$$

$$= \|\mathbb{E}_X[\mathbf{U}_\theta(X)]^{1/2} \mathbf{D}_\lambda \mathbf{D}_\lambda^{-1} \mathbf{D}_a \mathbf{W}\|_{S^q} \quad (56)$$

$$\leq \|\mathbb{E}_X[\mathbf{U}_\theta(X)]^{1/2} \mathbf{D}_\lambda\|_{op} \|\mathbf{D}_\lambda^{-1} \mathbf{D}_a \mathbf{W}\|_{S^q}. \quad (57)$$

Observe that

$$\|\mathbf{D}_\lambda \mathbb{E}_X[\mathbf{U}_\theta(X)] \mathbf{D}_\lambda\|_{op} = \max_{\|\mathbf{v}\|_2=1} \mathbf{v}^\top \mathbf{D}_\lambda \mathbb{E}_X[\mathbf{U}_\theta(X)] \mathbf{D}_\lambda \mathbf{v} \quad (58)$$

$$= \max_{\|\mathbf{v}\|_2=1} \sum_k \sum_j v_k \lambda_k v_j \lambda_j \mathbb{E}_X \left[ U(\mathbf{w}_k^\top X + b_k) U(\mathbf{w}_j^\top X + b_k) \right] \quad (59)$$

$$\leq \max_{\|\mathbf{v}\|_2=1} \sum_k \sum_j v_k \lambda_k v_j \lambda_j \quad (60)$$

$$= \max_{\|\mathbf{v}\|_2=1} \left( \mathbf{v}^\top \boldsymbol{\lambda} \right)^2 \leq 1, \quad (61)$$

where the last inequality is due to Cauchy–Schwarz. We have shown  $\|\mathbf{D}_\lambda \mathbb{E}_X[\mathbf{U}_\theta(X)] \mathbf{D}_\lambda\|_{op} \leq 1$ , which implies  $\|\mathbb{E}_X[\mathbf{U}_\theta(X)]^{1/2} \mathbf{D}_\lambda\|_{op} \leq 1$ . Combining this fact with the inequality above, we see that

$$\mathcal{M}\mathcal{V}(f, q) \leq \|\mathbf{D}_\lambda^{-1} \mathbf{D}_a \mathbf{W}\|_{S^q}. \quad (62)$$

Since this inequality is independent of the choice of  $\lambda$ , we have that for  $q = \frac{2}{L-1}$ ,

$$\mathcal{M}\mathcal{V}(f, q) \leq \inf_{\substack{\|\lambda\|_2=1 \\ \lambda>0}} \|\mathbf{D}_\lambda^{-1} \mathbf{D}_a \mathbf{W}\|_{S^q} = \Phi_L(\mathbf{D}_a \mathbf{W})^{L/2}. \quad (63)$$

Finally, since the above inequality holds independent of the choice of parameters  $\theta$  realizing  $f$ , we have

$$\mathcal{M}\mathcal{V}(f, q) \leq \inf_{\theta: f=h_\theta^{(2)}|_{\mathcal{X}}} \Phi_L(\mathbf{D}_a \mathbf{W})^{L/2} = R_L(f)^{L/2}, \quad (64)$$

and taking  $(2/L)$ -powers of both sides of this inequality gives the claim.  $\square$

### B.3 Proof of Corollaries to Theorem 1

*Proof of Corollary 1.* For ease of notation, denote  $\text{rank}_I(f)$  by  $r$ . By definition  $\sigma_r(f) > 0$ . For any  $L \geq 2$ ,

$$\mathcal{M}\mathcal{V}\left(f, \frac{2}{L-1}\right)^{2/L} = \left(\sum_{k=1}^d \sigma_k(f)^{\frac{2}{L-1}}\right)^{\frac{L-1}{L}} \geq r^{\frac{L-1}{L}} \sigma_r(f)^{\frac{2}{L}}.$$

By Theorem 1, it follows that

$$r^{\frac{L-1}{L}} \sigma_r(f)^{\frac{2}{L}} \leq R_L(f) \leq r^{\frac{L-2}{L}} R_2(f)^{2/L}. \quad (65)$$

The upper and lower bounds from Equation (65) both tend to  $r$  as  $L \rightarrow \infty$ , so  $R_L(f) \rightarrow \text{rank}_I(f)$ .  $\square$

*Proof of Corollary 2.* Let  $r_l$  and  $r_h$  denote the index ranks of  $f_l$  and  $f_h$ , respectively. Choose

$$L_0 := 1 + 2 \frac{\log R_2(f_l) - \frac{1}{2} \log r_l - \log \sigma_{r_h}(f_h)}{\log r_h - \log r_l}. \quad (66)$$

Then  $L > L_0$  implies

$$r_l^{\frac{L-2}{L}} R_2(f_l) < r_h^{\frac{L-1}{L}} \sigma_{r_h}(f_h) \leq \mathcal{M}\mathcal{V}\left(f_h, \frac{2}{L-1}\right). \quad (67)$$

By Theorem 1, it follows that  $R_L(f_l) < R_L(f_h)$ .  $\square$

### B.4 Existence of Index Rank-1 Interpolants

**Lemma 6.** *Given training pairs  $\{(\mathbf{x}_i, y_i)\}_{i=1}^n$  with  $\mathbf{x}_i \in \mathcal{X}$  and  $y_i \in \mathbb{R}$ , assume that  $\mathbf{x}_i \neq \mathbf{x}_j$  whenever  $i \neq j$ . Then there exists a function  $f \in \mathcal{N}_2(\mathcal{X})$  such that  $f(\mathbf{x}_i) = y_i$  for all  $i \in [n]$  and  $\text{rank}_I(f) = 1$ .*

*Proof.* Let  $\mathcal{W}$  denote the set of all  $\mathbf{w} \in \mathbb{R}^d$  such that  $\mathbf{w}^\top \mathbf{x}_i = \mathbf{w}^\top \mathbf{x}_j$  for some  $i \neq j$ . Let  $\mathbf{z}_1, \dots, \mathbf{z}_N$  be an enumeration of all difference vectors  $\mathbf{x}_i - \mathbf{x}_j$ ,  $i \neq j$ . We can write  $\mathcal{W}$  as the set of all  $\mathbf{w} \in \mathbb{R}^d$  such that  $\mathbf{w}^\top \mathbf{z}_k = 0$  for some  $k \in 1, \dots, N$ . Thus,  $\mathcal{W}$  is the union of  $N$  different hyperplanes  $\mathcal{W}_k$ , where  $\mathcal{W}_k = \{\mathbf{w} : \mathbf{w}^\top \mathbf{z}_k = 0\}$  is the hyperplane normal to  $\mathbf{z}_k$ . Each  $\mathcal{W}_k$  is a  $d - 1$  dimensional hyperplane in  $\mathbb{R}^d$  and therefore has Lebesgue measure zero. Hence, their finite union (i.e.,  $\mathcal{W}$ ) must have measure zero as well. We conclude that there is some  $\mathbf{w}_* \in \mathbb{R}^d \setminus \mathcal{W}$  such that  $\mathbf{w}_*^\top \mathbf{x}_i \neq \mathbf{w}_*^\top \mathbf{x}_j$  whenever  $i \neq j$ .

Consider a univariate function  $g : \mathbb{R} \rightarrow \mathbb{R}$  in  $\mathcal{N}_2(\mathbb{R})$  that interpolates the projected data pairs  $\{(\mathbf{w}_*^\top \mathbf{x}_i, y_i)\}_{i=1}^n$ . For example, we can choose  $g(t)$  to be the piecewise linear spline interpolant with knots at  $t_i = \mathbf{w}_*^\top \mathbf{x}_i$  that is constant for  $t < \min_i t_i$  and  $t > \max_i t_i$ . This function  $g$  can be written as a sum of finitely many ReLU units and so belongs to  $\mathcal{N}_2(\mathbb{R})$ . Define  $f \in \mathcal{N}_2(\mathcal{X})$  by  $f(\mathbf{x}) := g(\mathbf{w}_*^\top \mathbf{x})$ . Then  $f$  interpolates the original training pairs  $\{(\mathbf{x}_i, y_i)\}_{i=1}^n$ . Further, the weak gradient of  $f$  is  $\nabla f(\mathbf{x}) = g'(\mathbf{w}_*^\top \mathbf{x}) \mathbf{w}_*$  where  $g'$  is the weak derivative of  $g$ . This means that the expected gradient outer product of  $f$  is equal to the rank one matrix  $\mathbb{E}_X[g'(\mathbf{w}_*^\top X)^2] \mathbf{w}_* \mathbf{w}_*^\top$ . Therefore  $\text{rank}_J(f) = 1$ .  $\square$

## B.5 Proof of Theorem 2

We begin with a lemma about the singular value decay of  $\hat{f}_L$  which is straightforward to prove using algebraic manipulations of Theorem 1; see Appendix E.3.

**Lemma 7.** *Assume that  $\hat{f}_L$  is an  $R_L$ -minimal interpolant. Then for all  $t \in [d]$ ,*

$$\sigma_t(\hat{f}_L) \leq \min_{s \in [d]} \frac{\mathcal{I}_s(\mathcal{D})}{\sqrt{s}} \left(\frac{s}{t}\right)^{\frac{L-1}{2}}. \quad (68)$$

Using this lemma, we now prove Theorem 2.

*Proof.* Assume to the contrary that

$$\text{rank}_{I,\varepsilon}(\hat{f}_L) > \min_{s \in [d]} s \left(\frac{\mathcal{I}_s(\mathcal{D})}{\varepsilon \sqrt{s}}\right)^{\frac{2}{L-1}}. \quad (69)$$

Then there is some integer  $t$  with

$$t > \min_{s \in [d]} s \left(\frac{\mathcal{I}_s(\mathcal{D})}{\varepsilon \sqrt{s}}\right)^{\frac{2}{L-1}} \quad (70)$$

such that  $\sigma_t(\hat{f}_L) > \varepsilon$ . Rearranging Equation (70) and applying Lemma 7, we conclude that

$$\varepsilon > \min_{s \in [d]} \frac{\mathcal{I}_s(\mathcal{D})}{\sqrt{s}} \left(\frac{s}{t}\right)^{\frac{L-1}{2}} \geq \sigma_t(\hat{f}_L). \quad (71)$$

This is a contradiction, so

$$\text{rank}_{I,\varepsilon}(\hat{f}_L) \leq \min_{s \in [d]} s \left(\frac{\mathcal{I}_s(\mathcal{D})}{\varepsilon \sqrt{s}}\right)^{\frac{2}{L-1}}. \quad (72)$$

Finally, the floor function can be put inside the minimum because  $\text{rank}_{I,\varepsilon}(\hat{f}_L)$  is an integer.  $\square$

Finally, to prove the lower bound on the effective rank given in Theorem 2, we provide the following lemma, which shows that under mild conditions the sum of squared singular values of a minimum  $R_L$ -cost interpolant for any  $L \geq 2$  is uniformly bounded below by a constant depending only on the data. In particular, this result implies that the top singular value of a sequence of minimum  $R_L$ -cost interpolants cannot vanish as  $L \rightarrow \infty$ , and so the  $\varepsilon$ -effective index rank is always at least one for sufficiently small  $\varepsilon$ . The proof can be found in Appendix E.4.

**Lemma 8.** *Assume that  $\hat{f}_L$  is an  $R_L$ -minimal interpolant. Suppose that  $\Omega \subseteq \mathcal{X}$  is any open bounded set with  $C^1$  boundary such that  $\rho$  is uniformly bounded away from zero on  $\Omega$ . Then*

$$\sum_{k=1}^d \sigma_k(\hat{f}_L)^2 \geq C \frac{(\min_{c \in \mathbb{R}} \max_{i: \mathbf{x}_i \in \Omega} |y_i - c|)^{d+2}}{\mathcal{I}_1(\mathcal{D})^d} \quad (73)$$

where  $C > 0$  is a constant depending only on  $\Omega$ ,  $\rho$  and  $d$ . In particular, if  $\Omega$  contains two points  $\mathbf{x}_i, \mathbf{x}_j$  whose corresponding labels  $y_i, y_j$  are not equal, the lower bound is non-zero.

## C Generalizing to Vector-Valued Functions

While we focus on functions  $f : \mathcal{X} \rightarrow \mathbb{R}$ , our results can be naturally generalized to vector-valued functions  $f : \mathcal{X} \rightarrow \mathbb{R}^D$  with  $D > 1$ . In this setting, the  $L$ -layer representation cost  $R_L(f)$  is the minimal cost  $C_L(\theta) = \frac{1}{L} \left( \|\mathbf{A}\|_F^2 + \sum_{\ell=1}^{L-1} \|\mathbf{W}_\ell\|_F^2 \right)$  required to parameterize  $f$  over  $\mathcal{X}$  as  $f(\mathbf{x}) = \mathbf{A}^\top [\mathbf{W}_{L-1} \cdots \mathbf{W}_2 \mathbf{W}_1 \mathbf{x} + \mathbf{b}]_+ + \mathbf{c}$  where now  $\mathbf{A}$  is a  $D \times K$  matrix and  $\mathbf{c}$  is a vector in  $\mathbb{R}^D$ .

Given  $f : \mathcal{X} \rightarrow \mathbb{R}^D$ , consider a generalization of the EGOP matrix where  $d \times 1$  gradient vectors are replaced by  $D \times d$  Jacobian matrices:

$$\mathbf{C}_f := \mathbb{E}_X [Jf(X)^\top Jf(X)] = \int_{\mathcal{X}} Jf(\mathbf{x})^\top Jf(\mathbf{x}) \rho(\mathbf{x}) d\mathbf{x}. \quad (74)$$

We refer to this as the expected Jacobian Gram matrix (EJGM). We use the EJGM instead of the EGOP to define the index rank, principal subspace, singular values, and mixed variation of vector-valued functions  $f$ .

For example, consider  $f = [f_1, f_2]^\top$  where both component functions  $f_1, f_2 : \mathcal{X} \rightarrow \mathbb{R}$  have index-rank 1 with distinct principal subspaces  $\text{span}(\mathbf{v}_1)$  and  $\text{span}(\mathbf{v}_2)$ , respectively. It is straightforward to verify that  $\mathbf{C}_f = \mathbf{C}_{f_1} + \mathbf{C}_{f_2}$ . Using this fact, we can see that the principal subspace of  $f$  (i.e., range of  $\mathbf{C}_f$ ) is  $\text{span}(\mathbf{v}_1, \mathbf{v}_2)$  and the index-rank is 2; note that the active subspace of  $f$  is the *sum* of the principal subspaces of  $f_1$  and  $f_2$  instead of their *union*.

Using these modified definitions, all the results in Section 4 hold with only minor changes in their proofs. We conclude that minimizing the  $R_L$  cost in this setting promotes learning functions  $f$  where each component  $f_j$  for  $j = 1, \dots, D$  is nearly constant orthogonal to a universal low-dimensional subspace (universal in the sense that the subspace does not depend on  $j$ ) and is smooth along that subspace.

## D Extensions of Theorem 2

In this section, we extend Theorem 2 to interpolants that nearly minimize the  $R_L$  cost and to functions that nearly minimize the  $R_L$ -regularized empirical risk. The proofs of these extensions are only slight modifications of the proof of Theorem 2.

**Corollary 4** (Effective index ranks of near-minimal interpolants.). *Assume that  $\hat{f} \in \mathcal{N}_2(\mathcal{X})$  is nearly an  $R_L$ -minimal interpolant. That is,  $\hat{f}(\mathbf{x}_i) = y_i$  for all  $i \in [n]$ , and for some small constant  $\alpha \geq 0$ ,*

$$R_L(\hat{f}) \leq (1 + \alpha) \left( \inf_{f \in \mathcal{N}_2(\mathcal{X})} R_L(f) \text{ s.t. } f(\mathbf{x}_i) = y_i \forall i \in [n] \right). \quad (75)$$

Then given  $\varepsilon > 0$ , we have the following bound on the  $\varepsilon$ -effective index rank of  $\hat{f}$ :

$$\text{rank}_{I,\varepsilon}(\hat{f}) \leq \min_{1 \leq s \leq d} \left[ (1 + \alpha)^{\frac{L}{L-1}} s \left( \frac{\mathcal{I}_s(\mathcal{D})}{\varepsilon \sqrt{s}} \right)^{\frac{2}{L-1}} \right]. \quad (76)$$

The parameter  $\alpha$  in Corollary 5 controls how close  $\hat{f}$  is to being  $R_L$ -minimal; if  $\alpha = 0$ , then  $\hat{f}$  is exactly an  $R_L$ -minimal interpolant. In the next result,  $\alpha$  plays a similar role; it controls how close  $\hat{f}$  is to minimizing the regularized empirical risk.

**Corollary 5** (Effective index ranks of near-minimizers of the regularized risk.). *Assume that  $\hat{f} \in \mathcal{N}_2(\mathcal{X})$  (nearly) minimizes the  $R_L$ -regularized empirical  $\ell^2$  risk. That is, for some regularization parameter  $\lambda > 0$  and some small constant  $\alpha \geq 0$*

$$\frac{1}{n} \sum_{i=1}^n |y_i - \hat{f}(\mathbf{x}_i)|^2 + \lambda R_L(\hat{f}) \leq (1 + \alpha) \left( \inf_{f \in \mathcal{N}_2(\mathcal{X})} \frac{1}{n} \sum_{i=1}^n |y_i - f(\mathbf{x}_i)|^2 + \lambda R_L(f) \right). \quad (77)$$

Then given  $\varepsilon > 0$ , we have the following bound on the  $\varepsilon$ -effective index rank of  $\hat{f}$ :

$$\text{rank}_{I,\varepsilon}(\hat{f}) \leq \min_{1 \leq s \leq d} \left[ (1 + \alpha)^{\frac{L}{L-1}} s \left( \frac{\mathcal{I}_s(\mathcal{D})}{\varepsilon \sqrt{s}} \right)^{\frac{2}{L-1}} \right]. \quad (78)$$

The proofs of Corollaries 4 and 5 are essentially identical to the proof of Theorem 2, but use a slightly modified version of Lemma 7, as follows.

**Lemma 9.** *Assume that  $\hat{f}$  satisfies Equation (75) or Equation (77). Then for all  $t \in [d]$ ,*

$$\sigma_t(\hat{f}) \leq (1 + \alpha)^{\frac{L}{2}} \min_{s \in [d]} \frac{\mathcal{I}_s(\mathcal{D})}{\sqrt{s}} \left( \frac{s}{t} \right)^{\frac{L-1}{2}}. \quad (79)$$

The proof of this lemma is given in Appendix E.3.

## E Additional Proofs and Lemmas for Results in Section 4

### E.1 Proof of Lemma 4

*Proof.* If  $f \in \mathcal{N}_2(\mathcal{X})$ , then  $f$  is a continuous piecewise linear function with finitely many linear regions. Let  $\Omega_1, \dots, \Omega_N \subseteq \mathcal{X}$  denote a disjoint partition of  $\mathcal{X}$  so that  $f$  is piecewise linear over each  $\Omega_j$  and each  $\Omega_j$  has positive measure. Let  $\chi_{\Omega_j}$  denote the indicator function for  $\Omega_j$ . There exist some  $\mathbf{v}_j \in \mathbb{R}^d$  and  $c_j \in \mathbb{R}$  for  $j = 1, \dots, N$  such that  $f(\mathbf{x}) = \sum_{j=1}^N (\mathbf{v}_j^\top \mathbf{x} + c_j) \chi_{\Omega_j}(\mathbf{x})$  for all  $\mathbf{x} \in \mathcal{X}$ . Observe that  $\nabla f(\mathbf{x}) = \sum_j \mathbf{v}_j \chi_{\Omega_j}(\mathbf{x})$  is the weak gradient of  $f(\mathbf{x})$ . Since each  $\Omega_j$  has positive measure, we see that  $\nabla f(\mathbf{x})^\top \mathbf{u} = 0$  for almost all  $\mathbf{x} \in \Omega_j$  implies  $\mathbf{v}_j^\top \mathbf{u} = 0$  for all  $j$ .



Now assume  $\mathbf{x}, \mathbf{x} + \mathbf{u} \in \mathcal{X}$ . Since  $\mathcal{X}$  is convex, for all  $t \in [0, 1]$  we have  $\mathbf{x} + t\mathbf{u} \in \mathcal{X}$ . Consider the cardinality of the range of the continuous function  $t \mapsto f(\mathbf{x} + t\mathbf{u})$ . First,

$$\begin{aligned} |\{f(\mathbf{x} + t\mathbf{u}) : t \in [0, 1]\}| &= \left| \left\{ \sum_{j=1}^N (\mathbf{v}_j^\top (\mathbf{x} + t\mathbf{u}) + c_j) \chi_{\Omega_j}(\mathbf{x} + t\mathbf{u}) : t \in [0, 1] \right\} \right| \\ &= \left| \left\{ \sum_{j=1}^N (\mathbf{v}_j^\top \mathbf{x} + c_j) \chi_{\Omega_j}(\mathbf{x} + t\mathbf{u}) : t \in [0, 1] \right\} \right| \end{aligned}$$

because  $f$  is the continuous version of the expression in the right-hand side; on the boundaries between regions, the expression in the right-hand side is equal to zero. Next, observe that

$$\left| \left\{ \sum_{j=1}^N (\mathbf{v}_j^\top \mathbf{x} + c_j) \chi_{\Omega_j}(\mathbf{x} + t\mathbf{u}) : t \in [0, 1] \right\} \right| \leq 2^N \quad (80)$$

because any term in the sum can take on one of two values. A continuous function with finite range and connected domain must be constant, so  $f(\mathbf{x}) = f(\mathbf{x} + t\mathbf{u})$  for all  $t \in [0, 1]$ . In particular,  $f(\mathbf{x}) = f(\mathbf{x} + \mathbf{u})$ .  $\square$

## E.2 Proof of Lemma 5 when $\mathcal{X}$ is a bounded convex set

As before, we need to show that for all  $\theta = (\mathbf{W}, \mathbf{a}, \mathbf{b}, c) \in \Theta_2$  such that  $f = h_\theta^{(2)}|_{\mathcal{X}}$ , there is some  $\theta' = (\mathbf{W}', \mathbf{a}', \mathbf{b}', c') \in \Theta_2$  such that  $f = h_{\theta'}^{(2)}|_{\mathcal{X}}$ ,  $\text{rank}_I(f) \geq \text{rank}(\mathbf{D}_{\mathbf{a}'} \mathbf{W}')$ , and  $\Phi_L(\mathbf{D}_{\mathbf{a}'} \mathbf{W}') \leq \Phi_L(\mathbf{D}_{\mathbf{a}} \mathbf{W})$ . When  $\mathcal{X} = \mathbb{R}^d$ , the new parameterization  $\theta'$  is obtained by projecting the weight matrix  $\mathbf{W}$  onto the range of  $\mathbf{C}_f$ . This is not quite enough when  $\mathcal{X}$  is a bounded convex set, primarily because of units whose active set boundaries are outside  $\mathcal{X}$ . Instead, the strategy in creating  $\theta'$  when  $\mathcal{X}$  is a bounded convex set is to combine the problematic units into one affine piece and then apply the following technical lemma:

**Lemma 10.** *Assume  $\mathcal{X}$  is convex and has nonempty interior. Suppose*

$$f(\mathbf{x}) = \sum_{k=1}^K a_k [\mathbf{w}_k^\top \mathbf{x} + b_k]_+ + \mathbf{v}^\top \mathbf{x} + c, \quad \forall \mathbf{x} \in \mathcal{X}. \quad (81)$$

*Assume that for every unit  $k \in [K]$ ,  $a_k \neq 0$  and the active set boundaries  $H_k = \{\mathbf{x} : \mathbf{w}_k^\top \mathbf{x} + b_k = 0\}$  are distinct and intersect the interior of  $\mathcal{X}$ . Then  $\mathbf{v} \in \text{range}(\mathbf{C}_f)$  and  $\mathbf{w}_k \in \text{range}(\mathbf{C}_f)$  for all  $k \in [K]$ .*

*Proof.* It suffices to show that  $\mathbf{w}_1, \dots, \mathbf{w}_K$  and  $\mathbf{v}$  lie in  $\text{null}(\mathbf{C}_f)^\perp$ , so we fix a vector  $\mathbf{u} \in \text{null}(\mathbf{C}_f)$  and show that  $\mathbf{u}$  is orthogonal to  $\mathbf{w}_1, \dots, \mathbf{w}_K$  and  $\mathbf{v}$ .

Fix a unit  $k \in [K]$ . First, we pick a point on the active set boundary  $H_k$ . Let  $\mathcal{X}^\circ$  denote the interior of  $\mathcal{X}$ . Since the active set boundaries all intersect  $\mathcal{X}^\circ$  and are distinct, there is an  $\mathbf{x}_k \in H_k \cap \mathcal{X}^\circ$  such that  $\mathbf{x} \notin H_j$  whenever  $j \neq k$ .

Next, we consider small perturbations of  $\mathbf{x}_k$  in the direction of  $\pm \mathbf{w}_k$ . Pick  $\varepsilon > 0$  sufficiently small so that  $\mathbf{x}_k \pm \varepsilon \mathbf{w}_k \in \mathcal{X}^\circ$  and  $\varepsilon |\mathbf{w}_j^\top \mathbf{w}_k| < |\mathbf{w}_j^\top \mathbf{x}_k + b_j|$  whenever  $j \neq k$ . This implies that

1.  $\mathbf{w}_k^\top(\mathbf{x}_k + \varepsilon\mathbf{w}_k) + b_k > 0$ ,
2.  $\mathbf{w}_k^\top(\mathbf{x}_k - \varepsilon\mathbf{w}_k) + b_k < 0$ , and
3.  $\text{sign}(\mathbf{w}_j^\top(\mathbf{x}_k \pm \varepsilon\mathbf{w}_k) + b_j) = \text{sign}(\mathbf{w}_j^\top\mathbf{x}_k + b_j)$  for all  $j \neq k$ .

Thus, the points  $\mathbf{x}_k \pm \varepsilon\mathbf{w}_k$  lie on opposite sides of  $H_k$ , and for  $j \neq k$ , the points  $\mathbf{x}_k \pm \varepsilon\mathbf{w}_k$  are on the same side of  $H_j$  as  $\mathbf{x}_k$ .

We now consider small perturbations of  $\mathbf{x}_k \pm \varepsilon\mathbf{w}_k$  in the direction of  $\mathbf{u}$ . Choose  $\delta > 0$  sufficiently small so that  $\mathbf{x}_k \pm \varepsilon\mathbf{w}_k + \delta\mathbf{u} \in \mathcal{X}^\circ$ ,  $\delta|\mathbf{w}_k^\top\mathbf{u}| < \varepsilon\|\mathbf{w}_k\|_2^2$ , and  $\delta|\mathbf{w}_j^\top\mathbf{u}| < |\mathbf{w}_j^\top(\mathbf{x}_k \pm \varepsilon\mathbf{w}_k) + b_j|$  whenever  $j \neq k$ . This guarantees that

1.  $\mathbf{w}_k^\top(\mathbf{x}_k + \varepsilon\mathbf{w}_k + \delta\mathbf{u}) + b_k > 0$ ,
2.  $\mathbf{w}_k^\top(\mathbf{x}_k - \varepsilon\mathbf{w}_k + \delta\mathbf{u}) + b_k < 0$ , and
3.  $\text{sign}(\mathbf{w}_j^\top(\mathbf{x}_k \pm \varepsilon\mathbf{w}_k + \delta\mathbf{u}) + b_j) = \text{sign}(\mathbf{w}_j^\top\mathbf{x}_k + b_j)$  for all  $j \neq k$ .

That is, for every unit  $j \in [K]$ , the points  $\mathbf{x}_k \pm \varepsilon\mathbf{w}_k + \delta\mathbf{u}$  are on the same side of  $H_j$  as  $\mathbf{x}_k \pm \varepsilon\mathbf{w}_k$ . Additionally, Lemma 4 implies that  $f(\mathbf{x}_k \pm \varepsilon\mathbf{w}_k + \delta\mathbf{u}) = f(\mathbf{x}_k \pm \varepsilon\mathbf{w}_k)$ .

Because of this, it is straightforward to verify that

$$0 = f(\mathbf{x}_k - \varepsilon\mathbf{w}_k + \delta\mathbf{u}) - f(\mathbf{x}_k - \varepsilon\mathbf{w}_k) = \sum_{\substack{j \in [K] \\ \mathbf{w}_j^\top\mathbf{x}_k + b_j > 0}} \delta a_j \mathbf{w}_j^\top \mathbf{u} + \delta \mathbf{v}^\top \mathbf{u}. \quad (82)$$

On the other hand,  $\mathbf{x}_k + \varepsilon\mathbf{w}_k + \delta\mathbf{u}$  and  $\mathbf{x}_k + \varepsilon\mathbf{w}_k$  are also active on unit  $k$ , and so

$$0 = f(\mathbf{x}_k + \varepsilon\mathbf{w}_k + \delta\mathbf{u}) - f(\mathbf{x}_k + \varepsilon\mathbf{w}_k) = \sum_{\substack{j \in [K] \\ \mathbf{w}_j^\top\mathbf{x}_k + b_j \geq 0}} \delta a_j \mathbf{w}_j^\top \mathbf{u} + \delta \mathbf{v}^\top \mathbf{u}. \quad (83)$$

Subtracting Equation (82) from Equation (83) yields  $0 = \delta a_k \mathbf{w}_k^\top \mathbf{u}$ . Hence,  $\mathbf{w}_k^\top \mathbf{u} = 0$ . Since  $\mathbf{u}$  was arbitrary, we get  $\mathbf{w}_k \in \text{null}(\mathbf{C}_f)^\perp$ . Since this holds for all  $k \in [K]$ , it follows from (83) that  $\mathbf{v}$  lies in  $\text{null}(\mathbf{C}_f)^\perp$  as well.  $\square$

Using Lemma 10, we now finish the proof of Lemma 5 when  $\mathcal{X}$  is a bounded convex set by choosing a suitable  $\theta'$ .

*Proof.* If  $\mathcal{X}$  is a bounded convex set, we rewrite the parameterization

$$f(\mathbf{x}) = h_\theta^{(2)}(\mathbf{x}) = \sum_{k=1}^K a_k [\mathbf{w}_k^\top \mathbf{x} + b_k]_+ + c, \quad \forall \mathbf{x} \in \mathcal{X}. \quad (84)$$

in a way that allows us to apply Lemma 10. For convenience, we assume without loss of generality that  $\|\mathbf{w}_k\|_2 = 1$  for all  $k$ . (We may always rescale  $a_k$  and  $\mathbf{w}_k$  to ensure that this is true without changing the matrix  $\mathbf{D}_a \mathbf{W}$ .) We consider several types of units in  $\theta$ , and partition  $[K]$  accordingly as follows.

- $\Gamma_1 = \{k \in [K] : H_k \cap \mathcal{X}^\circ \neq \emptyset\}$ : These units have active sets that intersect the interior of  $\mathcal{X}$  and can be combined into units with distinct active set boundaries plus an affine term.

- $\Gamma_2 = \{k \in [K] : \mathbf{w}_k^\top \mathbf{x} + b_k \geq 0 \forall \mathbf{x} \in \mathcal{X}\}$ : These units are active on the entirety of  $\mathcal{X}$  and so can be combined into an affine term.
- $\Gamma_3 = \{k \in [K] : \mathbf{w}_k^\top \mathbf{x} + b_k \leq 0 \forall \mathbf{x} \in \mathcal{X}\}$ : These units are active on none of  $\mathcal{X}$  and so are immediately discarded.

We further distinguish between different units in  $\Gamma_1$  based on which ones share an active set boundary, whether units that share an active set boundary cancel out, and which side of shared active set boundaries are active. Formally, define the equivalence relation  $\sim$  on  $\Gamma_1$  by  $j \sim k$  if  $H_k = H_j$ . Each equivalence class modulo  $\sim$  contains units that share an active set boundary. Define

- $\Gamma_1^0 = \{k \in \Gamma_1 : \sum_{j \sim k} a_j = 0\}$
- $\Gamma_1^1 = \{k \in \Gamma_1 : \sum_{j \sim k} a_j \neq 0\}$

We denote the set of equivalence classes of  $\Gamma_1^1$  modulo  $\sim$  by  $\Gamma_1^1 / \sim$ . Let  $T^1$  be a transversal of  $\Gamma_1^1 / \sim$ . Since the weights  $\mathbf{w}_k$  are all normalized so that  $\|\mathbf{w}_k\|_2 = 1$ , note that  $j \sim k$  if and only if  $(\mathbf{w}_j, b_j) = \pm(\mathbf{w}_k, b_k)$ . To distinguish between the  $(\mathbf{w}_j, b_j) = (\mathbf{w}_k, b_k)$  and  $(\mathbf{w}_j, b_j) = (-\mathbf{w}_k, -b_k)$  cases, we write

- $\Gamma_1^{1+} = \{j \in \Gamma_1^1 : (\mathbf{w}_j, b_j) = (\mathbf{w}_k, b_k) \text{ for some } k \in T^1\}$
- $\Gamma_1^{1-} = \{j \in \Gamma_1^1 : (\mathbf{w}_j, b_j) = (-\mathbf{w}_k, -b_k) \text{ for some } k \in T^1\}$

We similarly define  $T^0$ ,  $\Gamma_1^{0+}$  and  $\Gamma_1^{0-}$ .

Now given  $\mathbf{x} \in \mathcal{X}$ , we use the identity  $[-t]_+ = [t]_+ - t$  to see that

$$\sum_{k \in \Gamma_1^1} a_k [\mathbf{w}_k^\top \mathbf{x} + b_k]_+ = \sum_{k \in T^1} \sum_{j \sim k} a_j [\mathbf{w}_j^\top \mathbf{x} + b_j]_+ \quad (85)$$

$$= \sum_{k \in T^1} \left( \sum_{\substack{j \sim k \\ \mathbf{w}_j = \mathbf{w}_k}} a_j [\mathbf{w}_k^\top \mathbf{x} + b_k]_+ + \sum_{\substack{j \sim k \\ \mathbf{w}_j = -\mathbf{w}_k}} a_j [-\mathbf{w}_k^\top \mathbf{x} - b_k]_+ \right) \quad (86)$$

$$= \sum_{k \in T^1} \left( \sum_{j \sim k} a_j [\mathbf{w}_k^\top \mathbf{x} + b_k]_+ - \sum_{\substack{j \sim k \\ \mathbf{w}_j = -\mathbf{w}_k}} a_j (\mathbf{w}_k^\top \mathbf{x} + b_k) \right) \quad (87)$$

$$= \left( \sum_{k \in T^1} \sum_{j \sim k} a_j [\mathbf{w}_k^\top \mathbf{x} + b_k]_+ \right) + \sum_{j \in \Gamma_1^{1-}} a_j \mathbf{w}_j^\top \mathbf{x} + C \quad (88)$$

where  $+C$  denotes a term that is constant with respect to  $\mathbf{x}$ .<sup>3</sup> A nearly identical derivation shows that

$$\sum_{k \in \Gamma_1^0} a_k [\mathbf{w}_k^\top \mathbf{x} + b_k]_+ = \sum_{j \in \Gamma_1^{0-}} a_j \mathbf{w}_j^\top \mathbf{x} + C. \quad (89)$$

---

<sup>3</sup>Note that the value of  $C$  may change from line to line in this proof.

Additionally, since the units in  $\Gamma_2$  are active on the entirety of  $\mathcal{X}$ ,

$$\sum_{k \in \Gamma_2} a_k [\mathbf{w}_k^\top \mathbf{x} + b_k]_+ = \sum_{k \in \Gamma_2} a_k \mathbf{w}_k^\top \mathbf{x} + C. \quad (90)$$

Using Equations (88) to (90), we rewrite Equation (84) as follows:

$$f(\mathbf{x}) = \sum_{k \in T^1} \left( \sum_{j \sim k} a_j \right) [\mathbf{w}_k^\top \mathbf{x} + b_k]_+ + \sum_{k \in \Gamma_1^{0-} \cup \Gamma_1^{1-} \cup \Gamma_2} a_k \mathbf{w}_k^\top \mathbf{x} + C, \quad \forall \mathbf{x} \in \mathcal{X}. \quad (91)$$

Lemma 10 applies to this form and tells us that the vectors  $\mathbf{w}_k$  for  $k \in T^1$  lie in the range of  $\mathbf{C}_f$ . For any  $j \in \Gamma_1^1$ , the vector  $\mathbf{w}_j$  is co-linear with some vector  $\mathbf{w}_k$  with  $k \in T^1$ , and so  $\mathbf{w}_j$  lies in the range of  $\mathbf{C}_f$  as well. Lemma 10 also tells us that the vector  $\sum_{k \in \Gamma_1^{0-} \cup \Gamma_1^{1-} \cup \Gamma_2} a_k \mathbf{w}_k$  lies in the range of  $\mathbf{C}_f$ . Since the vectors  $\mathbf{w}_k$  corresponding to  $\Gamma_1^{1-}$  are in the range of  $\mathbf{C}_f$ , we may subtract them from the sum. This allows us to conclude that  $\sum_{k \in \Gamma_1^{0-} \cup \Gamma_2} a_k \mathbf{w}_k$  is in the range of  $\mathbf{C}_f$ , though it is possible that some individual vectors in the sum are not.

The equation Equation (91) is very close to the parameterization  $\theta'$  that we want. However, it is convenient to ensure that the matrix  $\mathbf{D}_{\alpha'} \mathbf{W}'$  corresponds to a subset of the rows of  $\mathbf{D}_\alpha \mathbf{W} \mathbf{P}$  so that, similarly to the  $\mathcal{X} = \mathbb{R}^d$  case, we can establish that  $\text{rank}(\mathbf{D}_{\alpha'} \mathbf{W}') \leq \text{rank}_I(f)$  and  $\Phi_L(\mathbf{D}_{\alpha'} \mathbf{W}') \leq \Phi_L(\mathbf{D}_\alpha \mathbf{W})$ . Additionally, the parameterization  $h_{\theta'}^{(2)}$  must not include skip connections, so we need to convert the skip connection from Equation (91) into ReLU units. Since  $\mathcal{X}$  is bounded, there is some  $B \in \mathbb{R}$  such that  $\|\mathbf{x}\|_2 \leq B$  for all  $\mathbf{x} \in \mathcal{X}$ . Each  $\mathbf{w}_k$  term has norm 1, and so  $\mathbf{w}^\top \mathbf{P} \mathbf{x} + B \geq 0$  for all  $\mathbf{x} \in \mathcal{X}$ . Putting this all together with our knowledge that certain vectors lie in the range of  $\mathbf{C}_f$ , we use Equations (89) and (90) to observe that

$$f(\mathbf{x}) = \sum_{k \in \Gamma_1^1} a_k [\mathbf{w}_k^\top \mathbf{x} + b_k]_+ + \sum_{k \in \Gamma_1^{0-} \cup \Gamma_2} a_k \mathbf{w}_k^\top \mathbf{x} + C \quad (92)$$

$$= \sum_{k \in \Gamma_1^1} a_k [\mathbf{w}_k^\top \mathbf{P} \mathbf{x} + b_k]_+ + \sum_{k \in \Gamma_1^{0-} \cup \Gamma_2} a_k \mathbf{w}_k^\top \mathbf{P} \mathbf{x} + C \quad (93)$$

$$= \sum_{k \in \Gamma_1^1} a_k [\mathbf{w}_k^\top \mathbf{P} \mathbf{x} + b_k]_+ + \sum_{k \in \Gamma_1^{0-} \cup \Gamma_2} a_k [\mathbf{w}_k^\top \mathbf{P} \mathbf{x} + B]_+ + C \quad (94)$$

Choosing  $\theta'$  be this final parameterization from Equation (94) means that the matrix  $\mathbf{D}_{\alpha'} \mathbf{W}'$  corresponds to a subset of the rows of  $\mathbf{D}_\alpha \mathbf{W} \mathbf{P}$ , so  $\text{rank}(\mathbf{D}_{\alpha'} \mathbf{W}') \leq \text{rank}_I(f)$  and  $\Phi_L(\mathbf{D}_{\alpha'} \mathbf{W}') \leq \Phi_L(\mathbf{D}_\alpha \mathbf{W})$  just as in the proof of the  $\mathcal{X} = \mathbb{R}^d$  case.  $\square$

### E.3 Proofs of Lemma 7 and Lemma 9

*Proof.* Fix  $s, t \in [d]$ . The lower bound from Theorem 1 tells us that for any  $f \in \mathcal{N}_2(\mathcal{X})$ ,

$$R_L(f) \geq \mathcal{M}\mathcal{V} \left( f, \frac{2}{L-1} \right)^{2/L} = \left( \sum_{i=1}^d \sigma_i(f)^{\frac{2}{L-1}} \right)^{\frac{L-1}{L}} \geq t^{\frac{L-1}{L}} \sigma_t(f)^{\frac{2}{L}}. \quad (95)$$

On the other hand,

$$\inf_{f \in \mathcal{N}_2(\mathcal{X})} R_L(f) \quad \text{s.t.} \quad f(\mathbf{x}_i) = y_i \quad \forall i \in [n] \quad (96)$$

$$\leq \inf_{f \in \mathcal{N}_2(\mathcal{X})} R_L(f) \quad \text{s.t.} \quad f(\mathbf{x}_i) = y_i \quad \forall i \in [n] \quad \text{and} \quad \text{rank}_I(f) \leq s \quad (97)$$

$$\leq s^{\frac{L-2}{L}} \inf_{f \in \mathcal{N}_2(\mathcal{X})} R_2(f)^{2/L} \quad \text{s.t.} \quad f(\mathbf{x}_i) = y_i \quad \forall i \in [n] \quad \text{and} \quad \text{rank}_I(f) \leq s \quad (98)$$

$$= s^{\frac{L-2}{L}} \mathcal{I}_s(\mathcal{D})^{2/L} \quad (99)$$

where the second inequality comes from the upper bound in Theorem 1.

Now for Lemma 7, if  $\hat{f}$  is an  $R_L$ -minimal interpolant, then

$$R_L(\hat{f}) = \inf_{f \in \mathcal{N}_2(\mathcal{X})} R_L(f) \quad \text{s.t.} \quad f(\mathbf{x}_i) = y_i \quad \forall i \in [n]. \quad (100)$$

Using Equations (95) and (99), we may conclude that

$$t^{\frac{L-1}{L}} \sigma_t(\hat{f})^{\frac{2}{L}} \leq s^{\frac{L-2}{L}} \mathcal{I}_s(\mathcal{D})^{2/L}. \quad (101)$$

For Lemma 9, if  $\hat{f}$  satisfies Equation (75), then similarly Equations (95) and (99) imply that

$$t^{\frac{L-1}{L}} \sigma_t(\hat{f})^{\frac{2}{L}} \leq (1 + \alpha) s^{\frac{L-2}{L}} \mathcal{I}_s(\mathcal{D})^{2/L}. \quad (102)$$

If  $\hat{f}$  satisfies Equation (77) then,

$$\lambda R_L(\hat{f}) \leq \frac{1}{n} \sum_{i=1}^n |y_i - \hat{f}(\mathbf{x}_i)|^2 + \lambda R_L(\hat{f}) \quad (103)$$

$$\leq (1 + \alpha) \left( \inf_{f \in \mathcal{N}_2(\mathcal{X})} \frac{1}{n} \sum_{i=1}^n |y_i - f(\mathbf{x}_i)|^2 + \lambda R_L(f) \right) \quad (104)$$

$$\leq (1 + \alpha) \left( \inf_{\substack{f \in \mathcal{N}_2(\mathcal{X}) \\ f(\mathbf{x}_i) = y_i \quad \forall i \in [n]}} \frac{1}{n} \sum_{i=1}^n |y_i - f(\mathbf{x}_i)|^2 + \lambda R_L(f) \right) \quad (105)$$

$$= \lambda(1 + \alpha) \left( \inf_{\substack{f \in \mathcal{N}_2(\mathcal{X}) \\ f(\mathbf{x}_i) = y_i \quad \forall i \in [n]}} R_L(f) \right). \quad (106)$$

With Equations (95) and (99), this implies Equation (102) holds as well in this case. In all cases, Lemmas 7 and 9 follow from rearranging Equations (101) and (102), respectively, and minimizing over  $s$ .  $\square$

#### E.4 Proof of Lemma 8

The proof is a consequence of the following key lemma that lower bounds the sum of squares of the singular values of any Lipschitz continuous data interpolating function. Below we use  $\text{Lip}(f)$  to denote the minimum Lipschitz constant of  $f$  on  $\mathcal{X}$ , i.e., the infimum over all constants  $c \geq 0$  such that  $|f(\mathbf{x}) - f(\mathbf{y})| \leq c \|\mathbf{x} - \mathbf{y}\|$  for all  $\mathbf{x}, \mathbf{y} \in \mathcal{X}$ .

**Lemma 11.** *Let  $\Omega \subset \mathcal{X}$  be as in Lemma 8. Then for any Lipschitz function  $f : \mathcal{X} \rightarrow \mathbb{R}$  that interpolates the data (i.e.,  $f(\mathbf{x}_i) = y_i$  for all  $i$ ) we have*

$$\sum_{k=1}^d \sigma_k(f)^2 \geq C \frac{(\min_{c \in \mathbb{R}} \max_{i: \mathbf{x}_i \in \Omega} |y_i - c|)^{d+2}}{\text{Lip}(f)^d}, \quad (107)$$

where  $C > 0$  is a universal constant depending on  $\Omega$ ,  $\rho$ , and  $d$ , but independent of  $f$  and the data.

*Proof.* First, it is straightforward to verify that

$$\sum_{k=1}^d \sigma_k(f)^2 = \text{tr}(\mathbf{C}_{f,\rho}) = \int_{\mathcal{X}} \|\nabla f(\mathbf{x})\|_2^2 \rho(\mathbf{x}) d\mathbf{x}, \quad (108)$$

Also, by assumption, there exists a constant  $C_1 > 0$  such that  $\rho(\mathbf{x}) \geq C_1$  for all  $\mathbf{x} \in \Omega$ , and so

$$\int_{\mathcal{X}} \|\nabla f(\mathbf{x})\|_2^2 \rho(\mathbf{x}) d\mathbf{x} \geq C_1 \int_{\Omega} \|\nabla f(\mathbf{x})\|_2^2 d\mathbf{x}. \quad (109)$$

Hence, it suffices to lower bound  $\|\nabla f\|_{L^2(\Omega)}^2 = \int_{\Omega} \|\nabla f(\mathbf{x})\|_2^2 d\mathbf{x}$ .

Towards this end, define  $\bar{f}_{\Omega} = \frac{1}{|\Omega|} \int_{\Omega} f(\mathbf{x}) d\mathbf{x}$  where  $|\Omega|$  denotes the Lebesgue measure of  $\Omega$ . By a Sobolev inequality (see, e.g., [71] Section 5.6.2) we have

$$\|f - \bar{f}\|_{L^\infty(\Omega)} \lesssim_{\Omega,d} \|f - \bar{f}\|_{L^{d+2}(\Omega)} + \|\nabla f\|_{L^{d+2}(\Omega)}, \quad (110)$$

where the notation  $A \lesssim_{\Omega,d} B$  indicates  $A \leq CB$  for a universal constant  $C$  depending only on  $\Omega$  and  $d$ . Furthermore, by Poincaré's inequality (see, e.g., [71] Section 5.8.1), we have

$$\|f - \bar{f}\|_{L^{d+2}(\Omega)} \lesssim_{\Omega,d} \|\nabla f\|_{L^{d+2}(\Omega)}, \quad (111)$$

and so combining the two inequalities above gives

$$\|f - \bar{f}\|_{L^\infty(\Omega)} \lesssim_{\Omega,d} \|\nabla f\|_{L^{d+2}(\Omega)}. \quad (112)$$

Next, since  $2 < d+2 < \infty$ , an  $L^p$ -norm interpolation inequality gives

$$\|\nabla f\|_{L^{d+2}(\Omega)} \leq \|\nabla f\|_{L^2(\Omega)}^{\frac{2}{d+2}} \|\nabla f\|_{L^\infty(\Omega)}^{\frac{d}{d+2}}. \quad (113)$$

Also, since  $\Omega \subset \mathcal{X}$  we have  $\|\nabla f\|_{L^\infty(\Omega)} \leq \|\nabla f\|_{L^\infty(\mathcal{X})}$ , while Rademacher's Theorem gives  $\|\nabla f\|_{L^\infty(\mathcal{X})} = \text{Lip}(f)$ . Therefore, we have shown

$$\|f - \bar{f}\|_{L^\infty(\Omega)} \lesssim_{\Omega,d} \text{Lip}(f)^{\frac{d}{d+2}} \|\nabla f\|_{L^2(\Omega)}^{\frac{2}{d+2}}, \quad (114)$$

which implies

$$\frac{\|f - \bar{f}\|_{L^\infty(\Omega)}^{d+2}}{\text{Lip}(f)^d} \lesssim_{\Omega,d} \|\nabla f\|_{L^2(\Omega)}^2. \quad (115)$$

Finally, since  $f$  satisfies  $f(\mathbf{x}_i) = y_i$  for all  $i \in [n]$ , we have

$$\|f - \bar{f}\|_{L^\infty(\Omega)} \geq \max_{i: \mathbf{x}_i \in \Omega} |y_i - \bar{f}| \geq \min_{c \in \mathbb{R}} \max_{i: \mathbf{x}_i \in \Omega} |y_i - c| \quad (116)$$

Combining this inequality with the one above gives the claim.  $\square$

To finish the proof of Lemma 8, all that remains is to bound the Lipschitz constant of minimal  $R_L$ -cost interpolants. This is achieved with the next two lemmas.

**Lemma 12.** *Suppose  $f \in \mathcal{N}_2(\mathcal{X})$ . Then  $\text{Lip}(f) \leq R_2(f)$ .*

*Proof.* Suppose  $f(\mathbf{x}) = \sum_{k=1}^K a_k [\mathbf{w}_k^\top \mathbf{x} + b_k]_+ + c$  is any parameterization of  $f$  such that  $\|\mathbf{w}_k\| = 1$  for all  $k = 1, \dots, K$ . Then a weak gradient of  $f$  is given by

$$\nabla f(\mathbf{x}) = \sum_k U(\mathbf{w}_k^\top \mathbf{x} + b_k) a_k \mathbf{w}_k \quad (117)$$

where  $U(\cdot)$  is the unit step function. Also, for any  $\mathbf{x} \in \mathcal{X}$  we have

$$\|\nabla f\|_{L^\infty(\mathcal{X})} \leq \sum_k \|U(\mathbf{w}_k^\top \mathbf{x} + b_k) a_k \mathbf{w}_k\| \leq \sum_k |U(\mathbf{w}_k^\top \mathbf{x} + b_k)| |a_k| \|\mathbf{w}_k\| \leq \sum_k |a_k| \quad (118)$$

Therefore, by taking the infimum over all such parameterizations of  $f$ , and using the characterization of the  $R_2$ -cost given in (8), we see that

$$\|\nabla f\|_{L^\infty(\mathcal{X})} \leq R_2(f), \quad (119)$$

Finally, by Rademacher's Theorem, we have  $\text{Lip}(f) = \|\nabla f\|_{L^\infty(\mathcal{X})}$ , which gives the claim.  $\square$

**Lemma 13.** *Let  $\hat{f}$  be a minimum  $R_L$ -cost interpolant of the data  $\mathcal{D}$ . Then  $\text{Lip}(\hat{f}) \leq \mathcal{I}_1(\mathcal{D})$ .*

*Proof.* Let  $f_1$  be a minimum  $R_2$ -cost index-rank-one interpolant of the data  $\mathcal{D}$ , such that  $\mathcal{I}_1(\mathcal{D}) = R_2(f_1)$ . Since  $\hat{f}$  is a  $R_L$  cost minimizer, we have

$$R_L(\hat{f})^{L/2} \leq R_L(f_1)^{L/2} = R_2(f_1) = \mathcal{I}_1(\mathcal{D}) \quad (120)$$

where the equality  $R_L(f_1)^{L/2} = R_2(f_1)$  follows from Theorem 1 and noting that  $f_1$  has index-rank one. On the other hand, by Lemma 12 and theorem 1 we have

$$\text{Lip}(\hat{f}) \leq R_2(\hat{f}) \leq R_L(\hat{f})^{L/2}. \quad (121)$$

Combining the two inequalities above gives the desired result.  $\square$

Lemma 8 now follows directly from Lemma 11 with  $f = \hat{f}$  and using the bound  $\text{Lip}(\hat{f}) \leq \mathcal{I}_1(\mathcal{D})$  given in Lemma 13.

## F Details of Numerical Experiments

All code can be found at the following link:

<https://github.com/suzannastep/linearlayers>.

**Data generation process** We choose a universal training superset  $\{\mathbf{x}_i\}_{i=1}^{2048}$  where each  $\mathbf{x}_i \sim U([-1/2, 1/2])$ . For each  $r \in \{1, 2\}$ , we create an index-rank- $r$  function  $f$  as described in Section 5 where

- $\mathbf{V}$  ( $20 \times r$ ) is the first  $r$  columns of a random orthogonal matrix,
- $\mathbf{U}$  ( $21 \times r$ ) is the first  $r$  columns of a random orthogonal matrix,
- $\mathbf{\Sigma}$  ( $r \times r$ ) is a diagonal matrix with entries drawn from  $U([0, 100])$ ,
- $\mathbf{W} = \mathbf{U}\mathbf{\Sigma}\mathbf{V}^\top$  ( $21 \times 20$ ), and
- $\mathbf{a}$  and  $\mathbf{b}$  ( $21 \times 1$ ) are vectors with entries drawn from the standard normal distribution and  $U([-1/2, 1/2])$ , respectively.

Then for each label noise standard deviation  $\sigma \in \{0, 0.25, 0.5, 1\}$ , we create training pairs of the form  $\{(\mathbf{x}_i, f(\mathbf{x}_i) + \varepsilon_i)\}_{i=1}^{2048}$  where  $\varepsilon_i \sim N(0, \sigma^2)$ . We then create training sets of size  $n \in \{64, 128, \dots, 2048\}$  consisting of  $\{(\mathbf{x}_i, f(\mathbf{x}_i) + \varepsilon_i)\}_{i=1}^n$ . This ensures that samples in the training set of size 64 are a subset of the samples in the training set of size 128, etc.

**Training and hyperparameter tuning** For each index rank  $r$ , dataset size  $n$ , and label noise standard deviation  $\sigma$ , we train a model of the form (4) of depth  $L$  and with hidden-layer widths all equal to 1000, starting from PyTorch’s default initialization using Adam and the mean-squared error loss. We train with a learning rate of  $10^{-4}$  for 60,000 epochs with a weight decay ( $\ell_2$ -regularization) parameter of  $\lambda$  followed by 100 epochs with a learning rate of  $10^{-5}$  and no weight decay. This final training period without weight decay ensures the trained networks have small mean-squared error; all models have a final training MSE of no more than  $\sigma + 10^{-2}$ . The values of the  $\ell_2$ -regularization term throughout training are plotted in Figure 9.

We tune the hyperparameters of depth ( $L$ ) and  $\ell_2$ -regularization strength ( $\lambda$ ) on a validation set of size 2048 from the same distribution as the training set. We use hyperparameter ranges of  $L \in \{3, \dots, 9\}$  and  $\lambda \in \{10^{-3}, 10^{-4}, 10^{-5}\}$ . Models with no linear layers correspond to depth  $L = 2$ , for which we tune the hyperparameter  $\lambda$  in the same way.



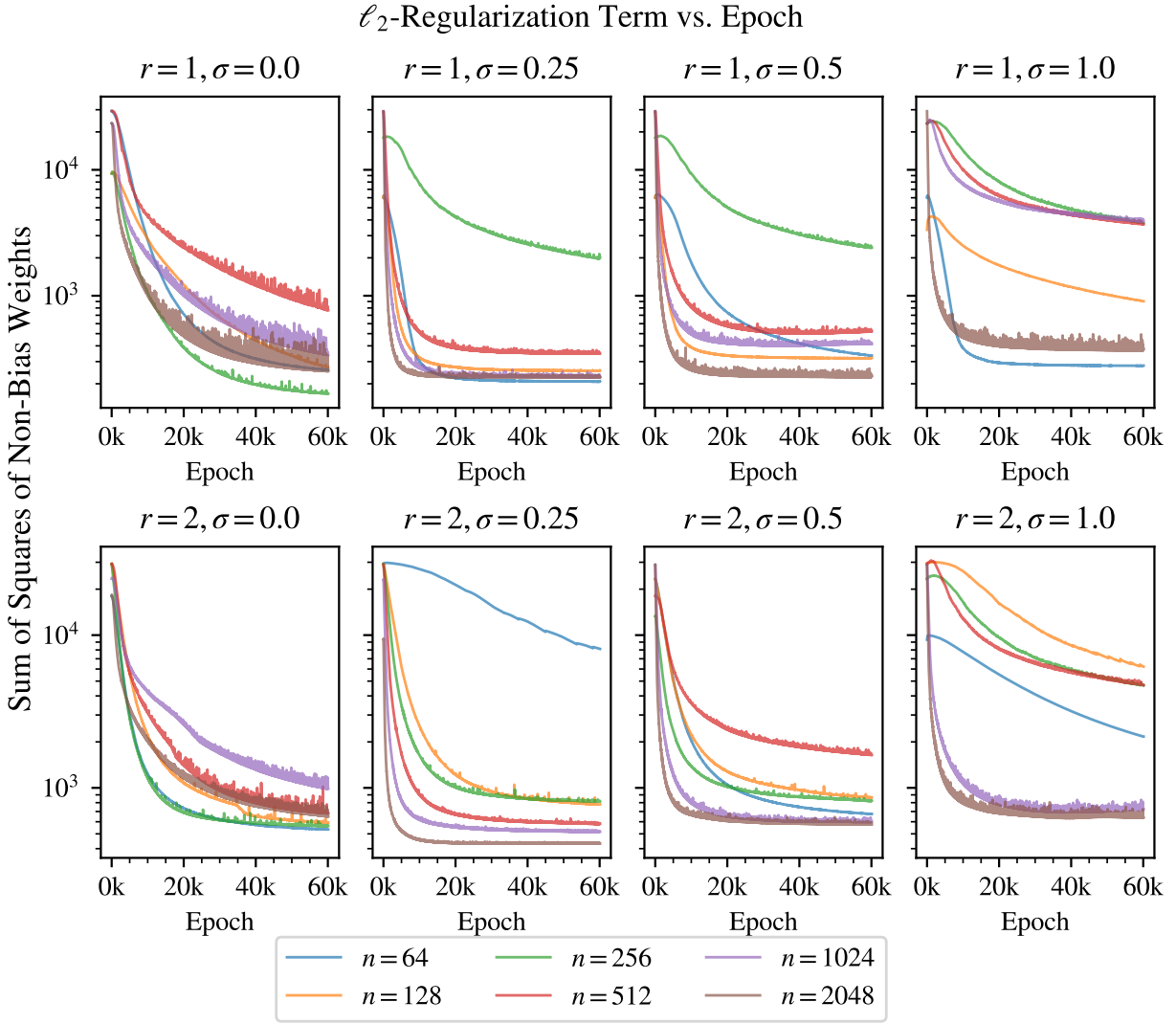


Figure 9: Values of the  $\ell_2$ -regularization term throughout 60,100 training epochs.